Geological Society of America Bulletin

# Mode and tempo of the Paleocene-Eocene thermal maximum in an expanded section from the Venetian pre-Alps

Luca Giusberti, Domenico Rio, Claudia Agnini, Jan Backman, Eliana Fornaciari, Fabio Tateo and Massimo Oddone

*Geological Society of America Bulletin* 2007;119, no. 3-4;391-412
doi: 10.1130/B25994.1

# Mode and tempo of the Paleocene-Eocene thermal maximum in an expanded section from the Venetian pre-Alps

**Luca Giusberti**†
*Department of Geology, Paleontology and Geophysics, Padova University, Via Giotto 1, I-35137 Padova, Italy*

**Domenico Rio**
*Department of Geology, Paleontology and Geophysics, Padova University, Via Giotto 1, I-35137 Padova, Italy, and Institute of Geosciences and Earth Resources, Consiglio Nazionale delle Ricerche (CNR) Padova, c/o Department of Geology, Paleontology and Geophysics, Padova University, Via Giotto 1, I-35137 Padova, Italy*

**Claudia Agnini**
*Department of Geology, Paleontology and Geophysics, Padova University, Via Giotto 1, I-35137 Padova, Italy*

**Jan Backman**
*Department of Geology and Geochemistry, Stockholm University, SE-106 91 Stockholm, Sweden*

**Eliana Fornaciari**
*Department of Geology, Paleontology and Geophysics, Padova University, Via Giotto 1, I-35137 Padova, Italy*

**Fabio Tateo**
*Institute of Geosciences and Earth Resources, Consiglio Nazionale delle Ricerche (CNR) Padova, c/o Department of Geology, Paleontology and Geophysics, Padova University, Via Giotto 1, I-35137 Padova, Italy*

**Massimo Oddone**
*Department of General Chemistry, University of Pavia, Via Taramelli 12, I-27100 Pavia, Italy*

## ABSTRACT

**The central part of the Piave River valley in the Venetian pre-Alps of NE Italy exposes an expanded and continuous marine sediment succession that encompasses the Paleocene series and the Paleocene to Eocene transition. The Paleocene through lowermost Eocene succession is >100 m thick and was deposited at middle to lower bathyal depths in a hemipelagic, near-continental setting in the central western Tethys. In the Forada section, the Paleocene succession of limestone-marl couplets is sharply interrupted by an ~3.30-m-thick unit of clays and marls (clay marl unit). The very base of this unit represents the biostratigraphic Paleocene-Eocene boundary, and the entire unit coincides with the main carbon isotope excursion of the Paleocene-Eocene thermal maximum event. Concentrations of hematite and biogenic carbonate, $\delta^{13}C$ measurements, and abundance of radiolarians, all oscillate in a cyclical fashion and are interpreted to represent precession cycles. The main excursion interval spans five complete cycles, that is, 105 ± 10 k.y. The overlying carbon isotope recovery interval, which is composed of six distinct limestone-marl couplets, is interpreted to represent six precessional cycles with a duration of 126 ± 12 k.y. The entire carbon isotope excursion interval in Forada has a total duration of ~231 ± 22 k.y., which is 5%–10% longer than previous estimates derived from open ocean sites (210–220 k.y.). Geochemical proxies for redox conditions indicate oxygenated conditions before, during, and after the carbon isotope excursion event. The Forada section exhibits a nonstepped sharp decrease in $\delta^{13}C$ (–2.35‰) at the base of the clay marl unit. The hemipelagic, near-continental depositional setting of Forada and the sharply elevated sedimentation rates throughout the clay marl unit argue for continuous rather than interrupted deposition and show that the initial nonstepped carbon isotope shift was not caused by a hiatus. A single sample at the base of the unit lacks biogenic carbonate. Preservation of carbonate thereafter improves progressively up-section in the clay marl unit, which is consistent with a prodigiously abrupt and rapid acidification of the oceans followed by a slower, successive deepening of the carbonate compensation depth. Increased sedimentation rates through the clay marl unit (approximately the main interval of the carbon isotope excursion) are consistent with an intensified hydrological cycle driven by supergreenhouse conditions and enhanced weathering and transport of terrigenous material to this near-continental, hemipelagic environment in the central western Tethys.**

**The sharp transition in lithology from the clay marl unit to the overlying limestone-marl couplets in the recovery interval and the coincident shift toward heavier $\delta^{13}C$ values suggest that the silicate pump and continental weathering, the cause of the enhanced terrigenous flux to Forada, stopped abruptly. This implies that the source of the light $CO_2$ ceased to be added to the ocean-atmosphere system at the top of the clay marl unit.**

**Keywords:** Paleocene-Eocene thermal maximum, carbon isotope record, central western Tethys, stratigraphy, geochemistry, mineralogy, chronology, silicate pump.

†E-mail: luca.giusberti@unipd.it.

*GSA Bulletin*; March/April 2007; v. 119; no. 3/4; p. 391–412; doi: 10.1130/B25994.1; 16 figures; 1 table; Data Repository item 2007029.

## INTRODUCTION

The Paleocene series was introduced by Schimper (1874). Over the years, it has become increasingly clear that the Paleocene represents a crucial interval of time in the Cenozoic Era for the evolution of the Earth system toward its present state. The base of the Paleocene corresponds to the last of the big five mass extinction events, the Cretaceous-Tertiary (K-T) boundary event, which was also characterized by a huge perturbation of the global carbon cycle (D'Hondt et al., 1998). The K-T boundary event was followed by recovery and reorganization of continental and marine faunas and floras during Paleocene times (Berggren et al., 1998; Gingerich, 2004). In the early late Paleocene, stable carbon isotope ($\delta^{13}C$) values in marine carbonates reached their heaviest values of the Cenozoic (e.g., Shackleton et al., 1985; Shackleton, 1987; Corfield and Cartlidge, 1992; Pak and Miller, 1992; Bralower et al., 1995; Thompson and Schmitz, 1997; Zachos et al., 2001). The end of the Paleocene is characterized by one of the largest Cenozoic disruptions in the global climatic system. Close to the Paleocene-Eocene boundary (Luterbacher et al., 2000), an extreme transient global warming event occurred (Kennett and Stott, 1991; Zachos et al., 1993); it is commonly referred to as the Paleocene-Eocene thermal maximum. The hallmark of the Paleocene-Eocene thermal maximum is a 2‰–4‰ global negative excursion in carbon isotopes, the carbon isotope excursion (CIE; Kennett and Stott, 1991; Koch et al., 1992). The carbon isotope excursion implies a rapid addition of huge (>2000 Gt) amounts of light carbon to the combined atmospheric and oceanic inorganic carbon reservoir (Dickens et al., 1995, 1997; Matsumoto, 1995; Zachos et al., 2005). The source and triggering mechanism of this event is still the focus of much debate (Cramer and Kent, 2005). A scenario in which successive blasts of biogenic methane derived from the marine gas hydrate reservoir (Dickens, 1999) has become the centerpiece of this debate.

Major biotic changes occurred at the Paleocene-Eocene thermal maximum. Benthic foraminifera suffered a severe extinction, the benthic extinction event (Tjalsma and Lohmann, 1983; Thomas and Shackleton, 1996; Thomas, 1998), mammals underwent the major turnover of their evolutionary history (Clyde and Gingerich, 1998; Gingerich, 2003), and pelagic biota were affected by major reorganizations (Bralower, 2002; Kelly, 2002; Raffi et al., 2005). The Paleocene-Eocene thermal maximum and carbon isotope excursion events have attracted much attention also because they are considered to represent an analogue in the geological past of the present-day rapid addition of greenhouse gases to the Earth system (Dickens, 1999).

In order to acquire a broader understanding of Earth system processes that characterized the Paleocene and the Paleocene-Eocene thermal maximum, it is necessary to expand the relatively sparse existing information across this interval with data from additional sediment sections representing a wide array of paleoenvironmental settings (Röhl et al., 2000). Efforts in this direction are currently being made in both continental and marine sedimentary archives. We report here on studies of the Paleocene series of the Venetian pre-Alps in NE Italy, which represents a middle latitude paleoenvironmental setting of the central western Tethys Seaway. During the Paleocene, this was a semirestricted oceanic area composed of shallow epicontinental seas surrounded by emergent land masses (Oberhänsli and Hsü, 1986; Oberhänsli, 1992).

The sections of the Venetian pre-Alps considered here are located in the central part of the Piave River valley, or Valbelluna. The expanded early Paleogene succession (Di Napoli Alliata et al., 1970; Costa et al., 1996) in this region is poorly documented in spite of the fact that it is one of the first localities where the benthic extinction event was recognized (Di Napoli Alliata et al., 1970). This paper presents three marine sections that encompass the Paleocene and lower Eocene from the Valbelluna region and show apparently continuous sedimentation across the Paleocene-Eocene thermal maximum interval. The Cicogna, Ardo, and Forada sections were all investigated using micropaleontological methods, whereas stable isotope and geochemical methods were added to Forada.

The continuously outcropping Forada section, which spans the terminal Cretaceous to the lower Eocene, contains a well-exposed and high-quality record of the Paleocene-Eocene thermal maximum. Geochemical and mineralogical data are presented at lower resolution for most of the Paleocene and at higher resolution across the Paleocene-Eocene thermal maximum. The still-controversial chronology of the carbon isotope excursion (Röhl et al., 2000; Cramer, 2001; Farley and Eltgroth, 2003) is discussed in the context of the paleoenvironmental setting of the central western Tethys Seaway. In addition, we document a shoaling of the carbonate compensation depth (CCD) at depths shallower than 1500 m at the base of the Paleocene-Eocene thermal maximum, thus adding evidence of the prodigious acidification of the oceans suggested by deep-sea drilling sites (Zachos et al., 2005).

## GEOLOGICAL SETTING

The Venetian pre-Alps are composed of a fold-and-thrust belt derived from the deformation of the African margin (Adria promontory) in the central Tethys Seaway (Channell et al., 1979); they are bounded by the Giudicarie and Insubric tectonic lines (Figs. 1A and 1B) and were affected by the Dinaric orogeny during the early Paleogene and by the Neoalpine orogeny during the Neogene (Doglioni and Bosellini, 1987). Tectonic deformations were less severe than elsewhere in the Alps and the Apennines (Channell and Medizza, 1981), making the pre-Alps suited for studies of the lower Paleogene pelagic record as exposed in its well-preserved sections.

The Mesozoic to early Cenozoic paleogeography of the pre-Alps was characterized by four NNE-SSW–trending plateaus and basins: from east to west, the Friuli Platform, the Belluno Basin, the Trento Plateau, and the Lombardian Basin (Fig. 1B) (Bernoulli and Jenkyns, 1974; Bernoulli et al., 1979; Winterer and Bosellini, 1981). This topography developed during late Paleozoic and Mesozoic rifting, thereby influencing sedimentation patterns. During Jurassic times, a regional drowning of the area led to widespread, rather uniform pelagic sedimentation within the entire Southern Alps (Channell et al., 1992); this ended in the early Paleogene, when the Veneto region changed into an articulated paleogeography that yielded various facies deposits, from continental to deep marine (Desio, 1974). Lower Paleogene deep-water sediments are particularly well developed in the NE-SW–oriented Belluno Basin, which was bordered to the west by the shallow Trento Plateau, the Lessini Shelf of Bosellini (1989), and to the south by shallow areas of the Friuli Platform (Fig. 1B).

In the Valbelluna area along the Piave River valley (Fig. 1C), up to 200–250-m-thick, Cretaceous to lower Eocene pelagic to hemipelagic sediments outcrop over a wide area and are overlain by a turbiditic sequence that can be up to 1000 m thick, called the Flysch di Belluno (Stefani and Grandesso, 1991; Costa et al., 1996; Fig. 2). These pelagic to hemipelagic sediments are mainly represented by well-bedded, pink to red limestones and marl limestones of Late Cretaceous to early Eocene age, which are often referred to as Scaglia Rossa. Variations in color and terrigenous content have been used to distinguish several formations within the Paleocene and lower Eocene Scaglia Rossa *Auctorum*: the Cugnan Formation, the Scaglia Cinerea, and the Marna della Vena d'Oro Formations (Di Napoli Alliata et al., 1970; Costa et al., 1996; Fig. 2). The Flysch di Belluno represents the lower Eocene foredeep deposits of the west-verging Dinaric thrusts (Doglioni and Bosellini, 1987).

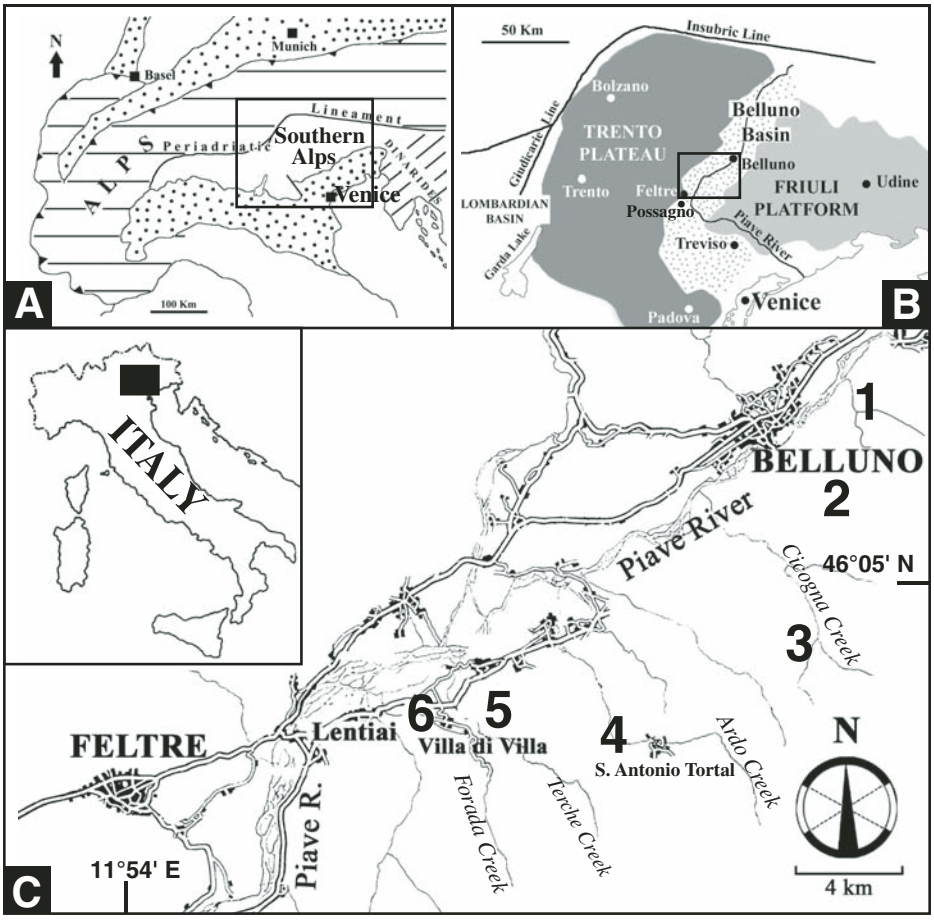


**Figure 1. Geographic and geological context of the Forada and other sections mentioned in the text. (A) Simplified geological scheme of the Southern Alps (adapted from Doglioni and Bosellini, 1987). (B) The main Late Cretaceous–early Paleogene paleogeographic elements of the Southern Alps (adapted from Cati et al., 1989). (C) The Piave River Valley in the Belluno Province (the "Valbelluna") showing location of the sections studied and mentioned in this work: 1—Vena d'Oro valley; 2—Madeago valley; 3—Cicogna Creek; 4—Ardo Creek; 5—Terche Creek; 6—Forada Creek.**

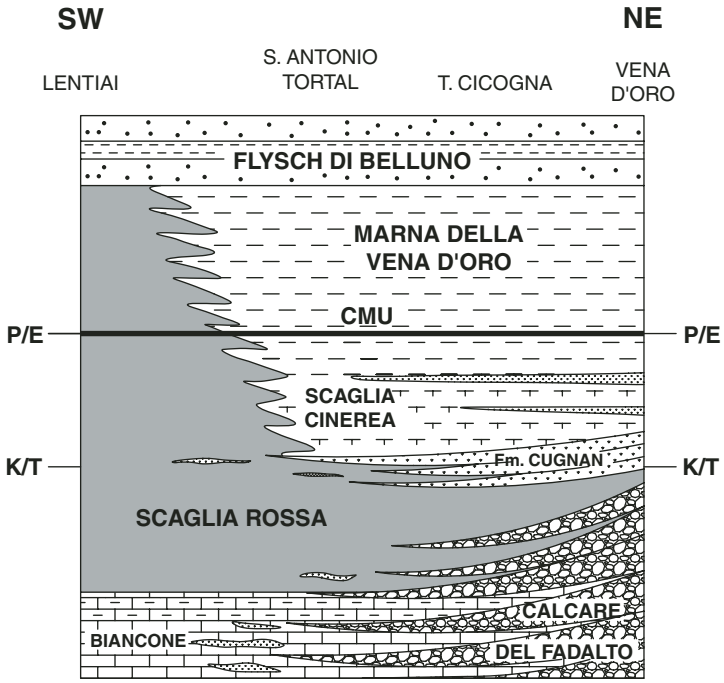


**Figure 2. Stratigraphic relationships of the Cretaceous and early Paleogene stratigraphic units of the Valbelluna. The Scaglia Rossa Formation in Valbelluna is up to 200–250 m thick. P/E—Paleocene-Eocene boundary; K/T—Cretaceous-Tertiary boundary.**

Structurally, the succession of the Belluno Basin forms a large, asymmetrical NE-SW–oriented syncline (Belluno syncline; Costa et al., 1996). The northern limb of the Belluno syncline, north of the Piave River, is strongly deformed by the Belluno line shear zone (Costa et al., 1996). The southern flank, south of the Piave River, is much less disturbed and hosts a series of west-flowing rivulets and creeks that cut deep into the Scaglia Rossa, roughly perpendicular to the strike, and expose virtually continuous sections of Upper Cretaceous to lower Eocene sediments in the Belluno Basin.

## MATERIALS AND METHODS

### Sections and Sampling

The Cicogna section is located along Cicogna Creek (Fig. 1C). The entire section is ~95 m thick (Fig. 3) and is here provisionally referred to as the Marna della Vena d'Oro Formation, except for the uppermost part, which has been ascribed to the Flysch di Belluno. Below the flysch, the lithology is represented by purple reddish, gray-greenish marls, with an upward increase of the terrigenous fraction. The section is continuously outcropping and is not affected by structural complications, except for an ~40-cm-thick interval at the Paleocene-Eocene boundary that shows signs of having been subjected to modest movement. The general bedding strike is 350°N, with a dip angle of ~10°.

The Ardo section is located along Ardo Creek, close to the S. Antonio Tortal village (Fig. 1C), and spans from the Upper Cretaceous to the lower Eocene (Costa et al., 1996). The portion of the Ardo succession considered here (Fig. 4) includes a basal part, ~20 m thick, composed of alternating pink-reddish limestone-marl limestone and abundant calciturbidites (Cugnan Formation). This unit is overlain by an ~10-m-thick interval of rhythmically organized gray marl limestone, here referred to as Scaglia Cinerea (Fig. 5A)[1], that, in turn, grades into gray-greenish, purple-reddish marls with an upwardly increasing amount of terrigenous material, here referred to as Marna della Vena d'Oro (Fig. 5B). The general strike is 340°N, and the dip is ~10°. The Paleocene part of the Ardo section that is used here (Fig. 4) shows negligible tectonic disturbances and is continuously outcropping.

The Forada section is located along Forada Creek, roughly 2 km east of the Lentiai village (Fig. 1C), and it consists of ~62 m of pink-reddish Scaglia Rossa limestones and marl limestones, locally rhythmically organized (Fig. 6). The Forada section also encompasses the interval from the Upper Cretaceous to the lower Eocene, outcrops continuously, and is virtually unaffected by structural complications. The general bedding strike is 350–355°N and the dip is 21–22°. A single tectonized interval has been observed in the lower Eocene, but faults or signs of deformation are lacking in the intervals spanning the K-T and the Paleocene-Eocene boundaries.

All three sections were initially sampled at low resolution for dating purposes using calcareous nannofossil biostratigraphy. When the biostratigraphic results indicated that the Forada section contained a good record of the K-T boundary and an expanded Paleocene-Eocene thermal maximum, a more detailed sampling was carried out there.

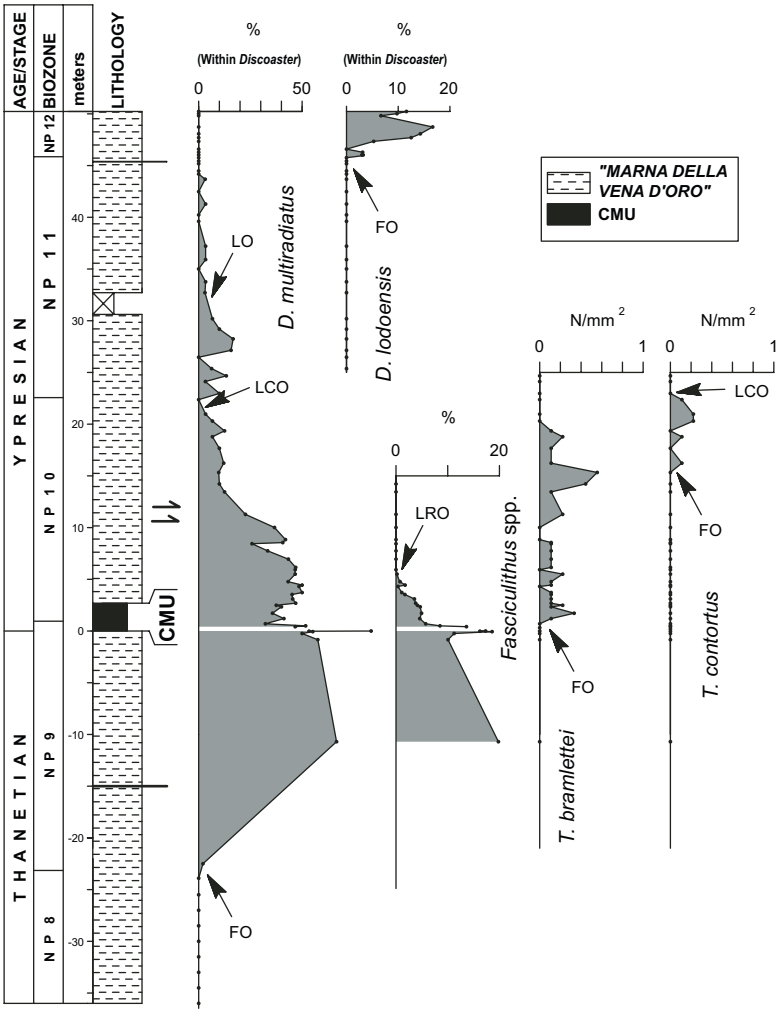


**Figure 3. Calcareous nannofossil biostratigraphy of the Cicogna section. FO—first occurrence; LO—last occurrence; LRO—last rare occurrence; LCO—last common and continuous occurrence. CMU—clay marl unit; *D.*—Discoaster; *T.*—Tribrachiatus.**

### Calcareous Nannofossils

Calcareous nannofossils were studied in smear-slides using light microscopy at 1250× or 1600× magnification. The taxonomy follows Perch-Nielsen (1985), and the zonal scheme is from Martini (1971), although lower Paleocene zones NP1-NP4 are combined. The first occurrence (FO) of *Cruciplacolithus primus* is well represented in the area (Agnini et al., 2005) and was used for correlation within the NP1-NP4 interval. The base of zone NP5 was approximated using the FO of the genus *Fasciculithus* rather than the formal definition, FO of *Fasciculithus tympaniformis*. Zones NP7 and NP8 cannot be differentiated because *Heliolithus riedelii* is missing in the material studied.

Different quantitative and semiquantitative techniques were employed for counting selected

[1]GSA Data Repository item 2007029, color versions of Figures 5 and 8 and results of chemical and isotopical analyses of the Forada section: $Ba_{biog}$, $CaCO_3$, $\delta^{13}C$, and $\delta^{18}O$, is available on the Web at http://www.geosociety.org/pubs/ft2007.htm. Requests may also be sent to editing@geosociety.org.

taxa, following Backman and Shackleton (1983), Rio et al. (1990), and Bralower (2002). The census data thus represent the following: (1) All sections: counts of a prefixed smear-slide area (specimens/mm$^2$); (2) Cicogna and Forada: counts of the index species relative to a prefixed number of taxonomically related forms (%) and counts of the total assemblage using 300–500 specimens (%); (3) Forada: members of *Coccolithus* and *Toweius* dominate the assemblages. Counts were continued until the number of specimens of all other taxa than *Coccolithus* and *Toweius* reached 200 specimens (%).

### Mineralogy and Geochemistry

For mineralogical analyses, semiquantitative estimates of crystalline phases were performed using an X-ray diffractometer (Miniflex Rigaku) equipped with a sample spinner and Cu tube, following Barahona (1974). Peak areas and positions were measured using the Winfit decomposition software (Krumm, 1994) and quartz as internal standard. Clay mineral analyses were conducted on the clay fraction (<2 µm) after carbonate removal at the Paleocene-Eocene transition in the Forada section. Semiquantitative estimates were based on Biscaye (1965), but slightly modified to account for the occurrence of mixed layers. The amount of the illitic component in the illite-smectite mixed layer was estimated according to Moore and Reynolds (1997).

For geochemical analyses, bulk samples were analyzed by X-ray fluorescence (Philips PW2400 spectrometer equipped with a Rh tube) using fused disks (1:10 rock:Li tetraborate ratio). Several international geologic standards were used for instrument calibration. The loss on ignition (LOI) was measured after heating the sample to 860 °C for 20 min and to 980 °C for 2 h, taking into account the content of divalent Fe. Permanganate titration was used to evaluate the concentration of divalent Fe.

The $Ba_{biog}$ values (Table DR1, see footnote 1) were calculated after Dymond et al. (1992) and are based on the $Ba/Al_2O_3$ ratio. The values represent barium in excess with respect to the composition of shales. The regression of CaO and $Al_2O_3$ suggests that the $Al_2O_3$ content of the clay component ranges from ~14% to 17%, which is in good agreement with the value of 15.11% compiled by Turekian and Wedepohl (1961).

Instrumental neutron activation analysis (INAA) was performed on the bulk rock of 23 samples according to the method described by Oddone et al. (1986).

Coulometry was used to determine calcium carbonate content (wt%). Analytical precision is within ±0.8%.

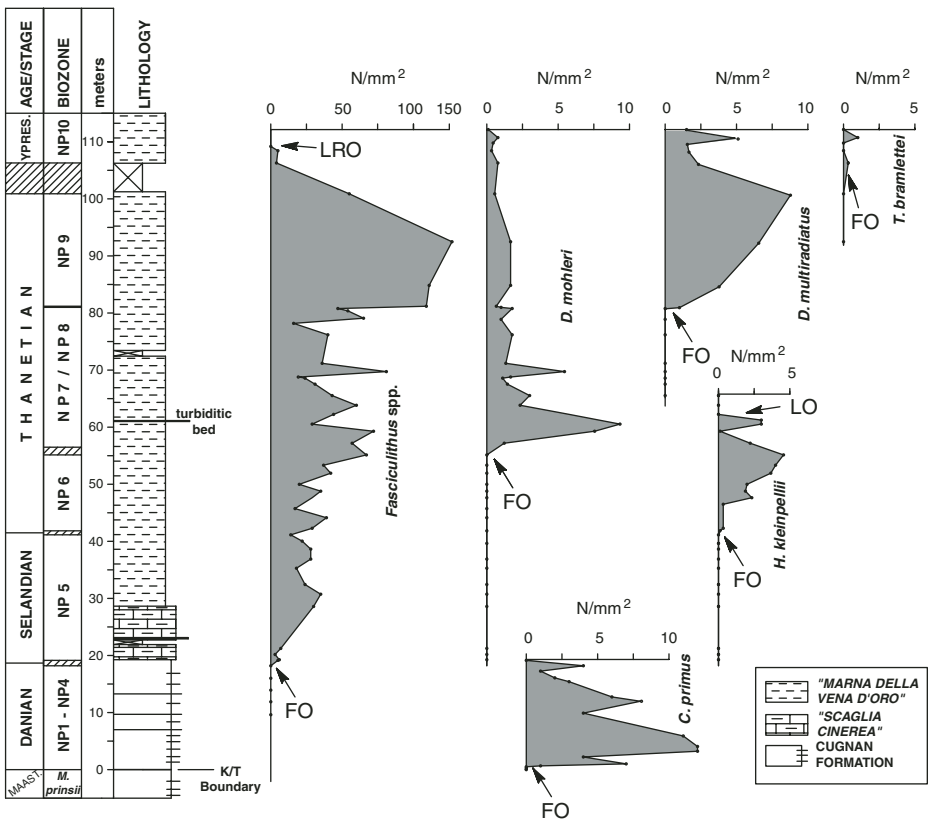


**Figure 4. Calcareous nannofossil biostratigraphy of the Ardo section. FO—first occurrence; LO—last occurrence; LRO—last rare occurrence. K/T—Cretaceous-Tertiary boundary; *M.—Micula*; *D.—Discoaster*; *H.—Heliolithus*; *C.—Cruciplacolithus*; *T.—Tribrachiatus*.**

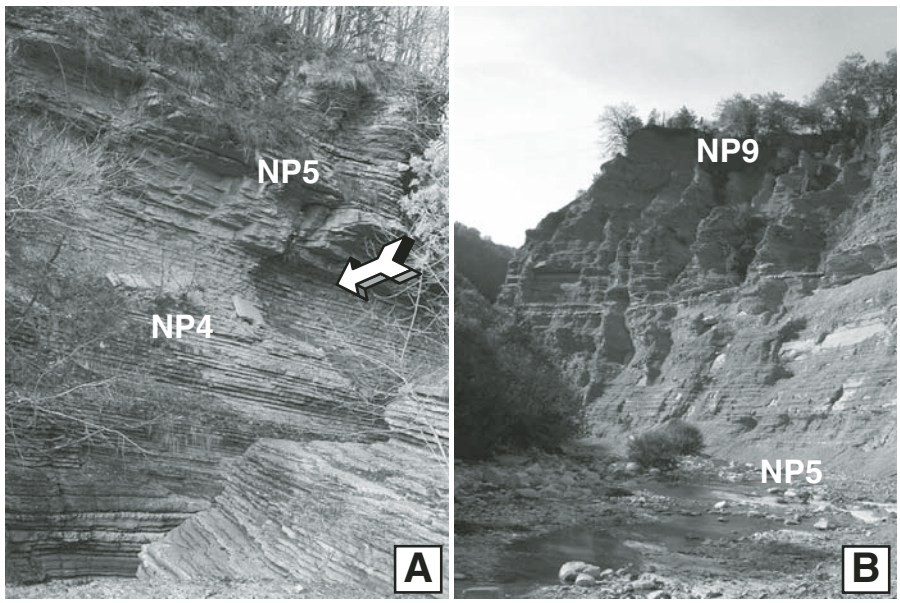


**Figure 5. Ardo section. (A) View of the Danian portion of the Cugnan Formation that outcrops close to the Ardo gorge ("Brent Grande"). The arrow indicates the first occurrence (FO) of *Fasciculithus* spp., which approximates the Danian-Selandian boundary (e.g., Schmitz et al., 1998). Total thickness of outcrop in photograph is ~20 m. (B) View of the Selandian and Thanetian (zone NP5 to zone NP9) in the Ardo section. Total thickness of outcrop in photograph is ~65 m.**

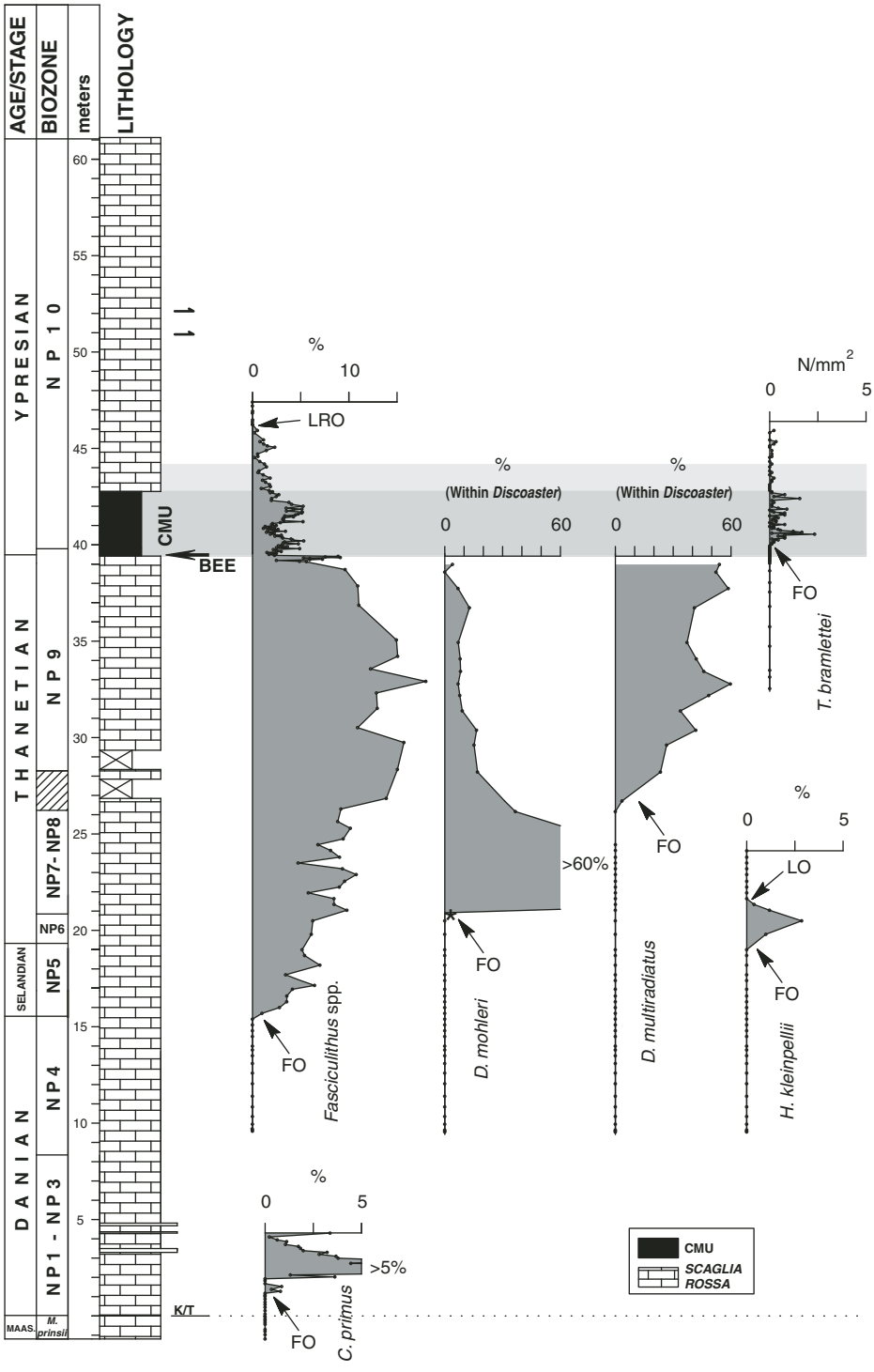


**Figure 6. Calcareous nannofossil biostratigraphy of the Forada section. FO—first occurrence; LO—last occurrence; LRO—last rare occurrence; BEE—benthic extinction event. CMU—clay marl unit; K/T—Cretaceous-Tertiary boundary; *M.—Micula*; *D.—Discoaster*; *H.—Heliolithus*; *C.—Cruciplacolithus*; *T.—Tribrachiatus*.**

Analytical data on $CaCO_3$ determined by recalculating chemical data and by coulometry are reported in Tables DR1 and DR2 (see footnote 1).

### Stable Isotopes

Nearly 170 bulk rock samples were analyzed for oxygen and carbon stable isotopes from the Forada section using a mass spectrometer (Finnigan MAT 252) equipped with a Kiel device. Carbon and oxygen isotopes values were calibrated to the Peedee belemnite standard (PDB) and converted to conventional delta notation ($\delta^{13}C$ and $\delta^{18}O$). Analytical precision is within ±0.06‰ for $\delta^{13}C$ and ±0.07‰ for $\delta^{18}O$. All the stable isotope data ($\delta^{13}C$ and $\delta^{18}O$) measured on bulk rock samples are reported in Table DR3 (see footnote 1).

### Organic Carbon

The organic carbon ($C_{org}$) was determined on carbonate-free residues of 23 samples, using a CE instruments EA 1110 automatic elemental analyzer equipped with AS 200 autosampler and Mettler Toledo AT21 comparator using a Ag crucible.

## PALEOCENE SERIES IN VALBELLUNA

Calcareous nannofossil biostratigraphies have been established for the Cicogna, Ardo, and Forada sections (Figs. 3, 4, and 6). Simplified columnar logs and critical biohorizons are shown together with correlation to the Possagno section (Agnini et al., 2006) in Veneto (Fig. 1B) and the Contessa Highway section in Umbria (Monechi and Thierstein, 1985; Fig. 7). The K-T boundary is preserved in the Ardo and Forada sections (Agnini et al., 2005), whereas the Paleocene to Eocene transition is well exposed only in the Forada and Cicogna sections.

Distinct Paleocene facies changes occur within all three sections because of upward-increasing contents of terrigenous material and westward-decreasing contents of redeposited shelf material, resulting in different thickness of correlative intervals (Fig. 7).

The Danian (approximately NP1–NP4) is represented by red carbonate lithofacies (Scaglia Rossa sensu stricto) with common calciturbidites in the Ardo Cugnan Formation (Figs. 4 and 5A), which are virtually missing in the westernmost Forada section, where only three, centimeter-scale calciturbiditic beds are observed (Fig. 6). The NP1–NP4 interval is condensed in the Valbelluna region, yet it is thicker in both the Ardo (18.8 m; 3.4 m/m.y.) and Forada (15.5 m; 2.8 m/m.y.) sections than

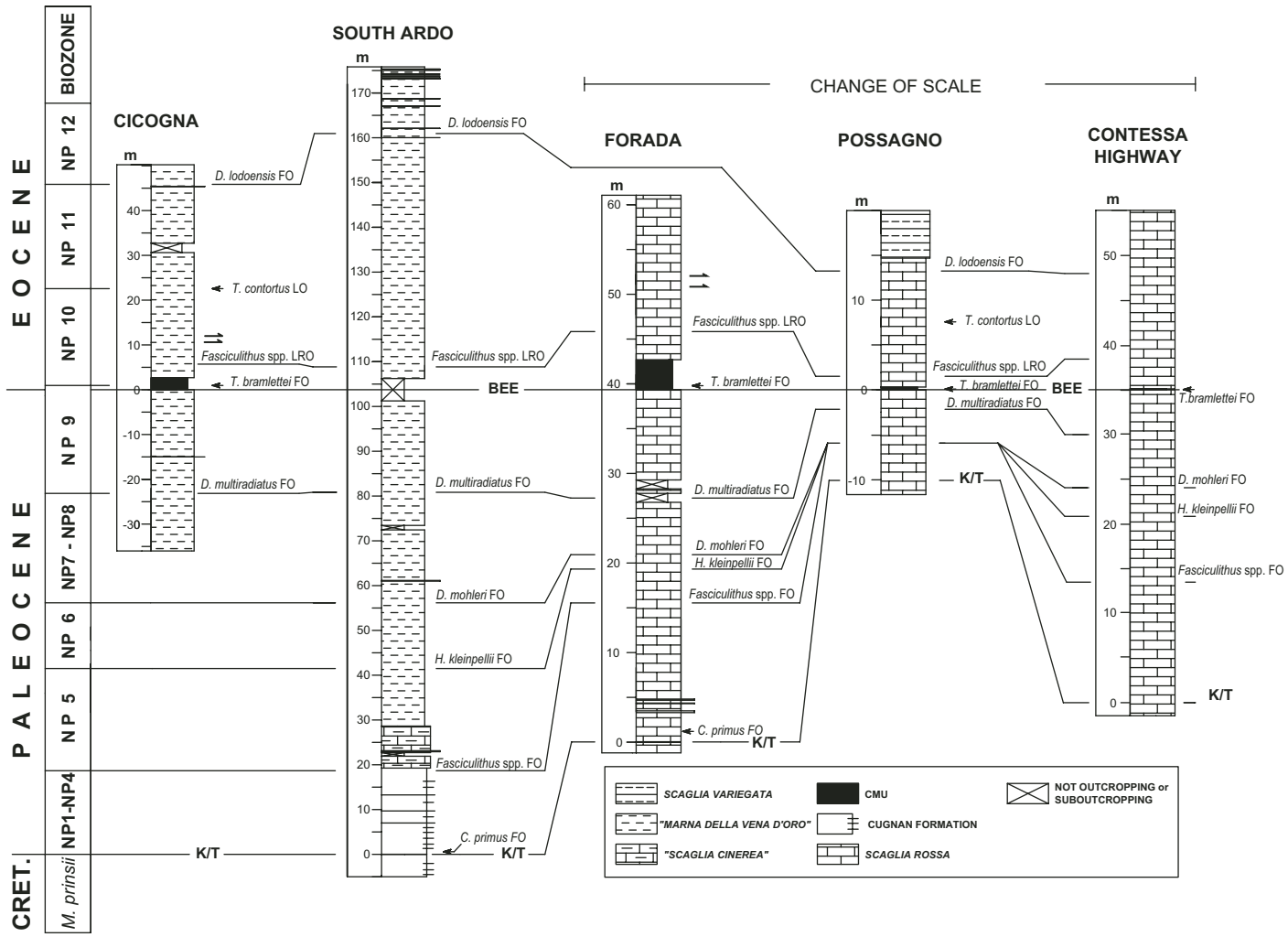


**Figure 7. The simplified stratigraphy of the sections studied here (located in Fig. 1) and correlation with the classical sections of Possagno (Veneto region) and the Contessa Highway (Umbria-Marche region, central Italy) based on calcareous nannofossil biostratigraphy. Data on Possagno section are after Agnini et al. (2006) and those on Contessa Highway are after Monechi and Thierstein (1985). Note the change of thickness scale to accommodate the vastly different linear sedimentation rates among sections. FO—first occurrence; LO—last occurrence; LRO—last rare occurrence; BEE—benthic extinction event; CMU—clay marl unit; K/T—Cretaceous-Tertiary boundary; *M.*—*Micula*; *D.*—*Discoaster*; *H.*—*Heliolithus*; *C.*—*Cruciplacolithus*; *T.*—*Tribrachiatus*.**

in the classical Contessa Highway section (13.4 m; 2.4 m/m.y.; Fig. 7).

The depositional regime changes throughout the basin at about the NP4–NP5 transition, approximating the Danian-Selandian boundary (Schmitz et al., 1998). This boundary is marked by the onset of Scaglia Cinerea deposition in Ardo (Figs. 5A and 7) and a concomitant decrease in carbonate content in Forada. Rates of sedimentation increased because of increased terrigenous input, the amount of which differed in various parts of the basin and hence resulted in different thicknesses of the NP5–NP9 intervals (Fig. 7). The Selandian–Thanetian interval is ~80 m thick (≈16 m/m.y.) in the Ardo section (Figs. 4, 5B, and 7).

The Paleocene and lower Eocene sediments in the Valbelluna sections show distinct lithologic cycles (Figs. 5A and 8, see footnote 1), commonly in the form of limestone-marlstone couplets, which presumably represent orbitally driven fertility cycles (Poletti et al., 2004).

The bulk mineralogy of the Forada section (Fig. 9) is dominated by calcite, except at the K-T boundary and within the clay marl unit (CMU). Other minerals present are sheet silicates, quartz, and feldspars. Calcite and the trace element barium show large variability (Fig. 9). Calcite content is characterized by a general decrease from the upper lower Paleocene through the upper Paleocene, reflecting the upward-increasing input of terrigenous material. Large fluctuations of calcite occur across the Paleocene-Eocene boundary and in the lower Eocene (Fig. 9). Biogenic barium shows a progressive increase throughout the Paleocene (Fig. 9), which is consistent with increasing productivity (Dymond et al., 1992; Paytan et al., 2002).

## CLAY MARL UNIT OF THE PALEOCENE-EOCENE THERMAL MAXIMUM IN VALBELLUNA

An easily recognized character of the lower Paleogene stratigraphy in Valbelluna is the 3–4-m-thick package of reddish and greenish marl clays and clayey marls, here referred to as the clay marl unit, that sharply interrupts

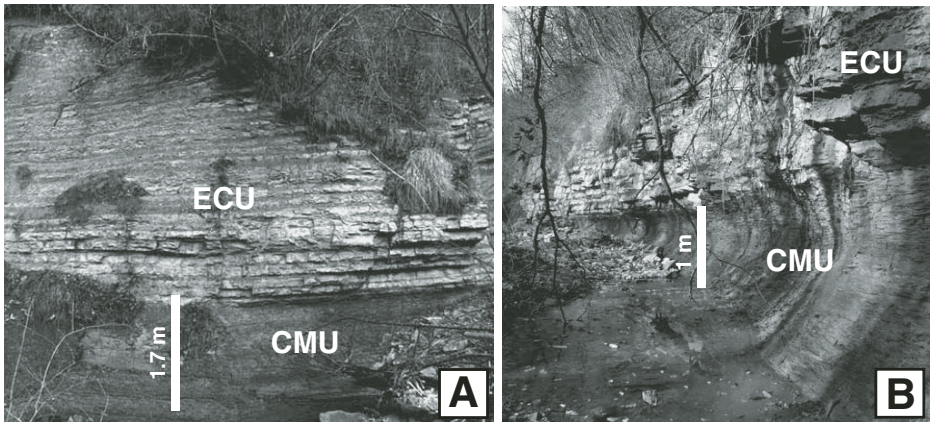


**Figure 8. Forada section: views of the well-developed early Eocene limestone-marl couplets (Eocene couplet unit—ECU) (A) and of the upper part of the clay marl unit (CMU) (B). The base of the clay marl unit corresponds to the onset of the carbon isotope excursion. The interval of low $\delta^{13}C$ has been recognized within the lithological anomaly, while the limestone-marl couplets represent the $\delta^{13}C$ recovery interval (see also Fig. 15).**

the previous carbonate sedimentation (Figs. 7–9). The clay marl unit is a pervasive feature in the Valbelluna region and has been observed in Cicogna (~2.7 m thick) and Forada (~3.3 m thick), but also in the Vena D'Oro Valley, the Madeago Valley, the Terche Valley (Fig. 1C), and in Possagno (Fig. 1B), albeit there reduced to ~30 cm thickness (Fig. 7; see also Arenillas et al., 1999; Agnini et al., 2006). This makes the clay marl unit an important lithostratigraphic correlation tool in the eastern Veneto region (Figs. 2 and 7).

Several independent data sets indicate that the clay marl unit is the lithologic expression of the Paleocene-Eocene thermal maximum in the Belluno basin. The evidence includes calcareous nannofossil biostratigraphy (Fig. 7), a major extinction event among benthic foraminifera (Figs. 6 and 7), presence of the calcareous nannofossil excursion taxa (Aubry et al., 2002), and the planktic foraminifera excursion taxa (Aubry et al., 2002). Moreover, bulk carbonate $\delta^{13}C$ and carbonate stratigraphies also support this inference.

Marine Paleocene-Eocene thermal maximum sections are typically clay-rich units. The clay marl unit of the Valbelluna is therefore analogous to the siliciclastic unit from Zumaya in Spain (Baceta et al., 2000; Schmitz et al., 2001), to the "recessive unit" in New Zealand sections (Hancock et al., 2003), and to several, virtually carbonate-free, clay-rich units observed in deep-sea settings (Moore et al., 1984; Norris et al., 1998; Bralower et al., 2002; Lyle et al., 2002; Zachos et al., 2004, 2005).

The number of available and continuous upper Paleocene–lower Eocene marine sediment sections is still relatively few (Röhl et al., 2000). Among the few continuous Paleocene-Eocene thermal maximum intervals available, Forada clearly is one of the most expanded so far described from a deep-marine setting (Table 1).

A prominent characteristic of the Paleocene–Eocene transition interval in Valbelluna is the lithologic cyclicity present below and above the clay marl unit (Fig. 8), consisting of couplets of reddish marls and indurate marl limestones (Eocene couplet unit). The transition between the clay marl unit and the nearest overlying marl limestone is sharp (Fig. 8).

## THE FORADA $\delta^{13}C$ PROFILE AND THE CARBON ISOTOPE EXCURSION

Shackleton and Hall (1984) published the first relatively detailed $\delta^{13}C$ profiles based on Paleocene and lower Eocene bulk sediment samples. These South Atlantic data provided a good overview of the large variability of Paleocene $\delta^{13}C$ in marine carbonate, displaying major features, trends, and 3‰–4‰ amplitude changes. Assessing whether or not consolidated to overconsolidated carbonates, such as those at Forada, faithfully record the global evolution of the carbon system is probably best accomplished through comparisons with other marine records (Corfield et al., 1991). The stratigraphically controlled trends and amplitude changes of the Forada $\delta^{13}C$ profile (Fig. 9) are strongly similar to a profile compiled from six South Atlantic Deep Sea Drilling Project (DSDP) sites (Shackleton, 1986, his Fig. 3). The Forada $\delta^{13}C$ profile is also compatible to profiles derived from other ocean basins, and hence to the global Paleocene $\delta^{13}C$ history (Shackleton et al., 1985; Corfield et al., 1991; Corfield, 1994; Schmitz et al., 1997b; Thompson and Schmitz, 1997; Zachos et al., 2001), indicating that diagenesis has not altered portions of the Forada $\delta^{13}C$ stratigraphy.

The Paleocene $\delta^{13}C$ maximum shows a value of about +2.5‰, which is somewhat lower than the ~3‰ observed in Contessa Highway section (Corfield et al., 1991) and in Zumaya (Schmitz et al., 1997b). But in agreement with the global trend, following the NP7-NP8 maximum, Forada shows a long-term $\delta^{13}C$ decrease throughout NP9 times (Kennett and Stott, 1990; Pak and Miller, 1992; Fig. 9). This long-term decline is interrupted by a prominent but transient negative shift (2.35‰) that occurs over a 12.5 cm interval across the base of the clay marl unit (Figs. 9 and 10) and is here interpreted as the carbon isotope excursion associated with the Paleocene-Eocene thermal maximum (Kennett and Stott, 1991; Röhl et al., 2000; Zachos et al., 2001).

The 2.35‰ $\delta^{13}C$ shift, from +0.48‰ to −1.87‰, of the basal carbon isotope excursion is somewhat lower in Forada compared to the 2.5‰ to 3‰ change generally reported in the literature for marine bulk carbonates (Kennett and Stott, 1991; Stott et al., 1996; Bralower et al., 1997; Katz et al., 1999; Dickens, 2001). Albian to Maastrichtian $\delta^{13}C$ values vary between +2‰ and +3‰ in red limestone bulk samples from the Umbrian Apennines (Corfield et al., 1991). The slightly heavier bulk sediment values in Forada are probably caused by the occurrence of relatively abundant, up to 20% (Fig. 10), reworked Cretaceous calcareous nannofossils in the clay marl unit, which presumably subdued the bulk sediment amplitude of the initial excursion in Forada.

Following the initial 2.35‰ $\delta^{13}C$ excursion over 12.5 cm across the base of the clay marl unit, values oscillate around an average of −0.8‰ from +25 cm, from the base of the clay marl unit, in a cyclical fashion up to +3.39 ± 0.14 m (Fig. 10). The interval from the initial negative excursion to the +3.4 m level represents the main body of the carbon isotope excursion, which coincides with the extension of the clay marl unit (Figs. 9 and 10). Above +3.39 ± 0.14 m, $\delta^{13}C$ values gradually return over an ~1.4 m interval to a new stable, average level of +0.9‰ beginning at +4.9 m and lasting throughout the remainder of Forada's lower Eocene succession. This recovery interval, representing an isotopic shift of 1.7‰, is a global phenomenon (Kennett and Stott, 1991; Bralower et al., 1997; Bains et al., 1999; Zachos et al., 2001, 2005). Another global character preserved in Forada is that the lower Eocene post–carbon isotope excursion (+0.9‰), or post–clay marl unit, $\delta^{13}C$ level is lighter than the upper Paleocene (NP6–NP9) pre–carbon isotope excursion level (+1.6‰) (Fig. 9).

TABLE 1. COMPARISON BETWEEN THE FORADA PALEOCENE-EOCENE THERMAL MAXIMUM AND OTHER REFERENCE SECTIONS

| Section | Location | Depositional environment | Lithological anomaly | Carbon isotope excursion thickness (bulk sample) | Remarks | References |
|---|---|---|---|---|---|---|
| Forada | NE Italy, Veneto region | Middle-lower bathyal | Clay marl unit: 3.3 m | ~4.80 m | | 1 |
| Possagno | NE Italy, Veneto region | Bathyal | Clay marl unit: 0.30 m | 0.50–0.65 m | | 2, 3 |
| Contessa Road | Central Italy, Umbria Marche | Middle-lower bathyal | Two intervals of marl: the lower marl is 0.12 m thick | 0.40 m | | 4, 5 |
| Untersberg | Austria | Lower bathyal | Claystone and marly claystone: 5.5 m | 5.50 m | | 6 |
| Alamedilla | Southern Spain | Lower bathyal | Marl clay: ~2.5 m | ~3.00 m | | 7, 8, 9 |
| Caravaca | Southern Spain | Middle bathyal | Two intervals of laminated shales: the lower shale is 2.5 m thick | ?8.00 m | $\delta^{13}C$ measured on single specimens of benthic foraminifera | 10, 11 |
| Zumaya | Basque countries, Spain | Middle-lower bathyal | Siliciclastic unit: 4 m of clay | ~5.45 m | Lower 1 m is devoid of original calcite | 12 |
| Trabakua | Basque countries, Spain | Lowermost middle bathyal | Very low carbonate content: 3.5 m of claystone | ?5.00 m | | 13, 14 |
| Dababiya | Southern Egypt | Outer shelf | Claystone/shale interval 2.68 m thick: the first 63 cm are carbonate-free | ~3.40 m | $\delta^{13}C$ measured on organic matter | 15, 16 |
| Sites 999/1001 | Caribbean Sea | Lower bathyal–upper abyssal | Claystone layer: 0.42 and 0.80 m, respectively | 0.50 and 2.50 m, respectively | | 17 |
| Site1263C/D | Walvis Ridge, southeastern Atlantic | Lower bathyal | Clay layer: 0.05 m | 1.95 m | | 18 |
| Mead Stream | New Zealand | Bathyal | Recessive unit (marly limestone and marl): 2.4 m | ~4.00 m | Critical interval is faulted at base | 19 |
| Site 690B | Weddell Sea | Lower bathyal | No detectable lithologic change: ~0.04 m of marl | 3.50 m | | 20, 21, 22 |

*Note:* (1) This work; (2) Arenillas et al. (1999); (3) Agnini et al. (2006); (4) Galeotti et al. (2000); (5) Galeotti et al. (2004); (6) Egger et al. (2005); (7) Lu et al. (1996); (8) Lu et al. (1998); (9) Molina et al. (1999); (10) Ortiz (1995); (11) Canudo et al. (1995); (12) Schmitz et al. (1997b); (13) Coccioni et al. (1994); (14) Orue-Extebarria et al. (1996); (15) Dupuis et al. (2003); (16) Alegret et al. (2005); (17) Bralower et al. (1997); (18) Zachos et al. (2005); (19) Hollis et al. (2005); (20) Bains et al. (1999); (21) Thomas et al. (1999); (22) Röhl et al. (2000).

## Forada Microstratigraphy across the Paleocene-Eocene Thermal Maximum

The Paleocene-Eocene transition at Forada is characterized not only by changes in carbonate content, $\delta^{13}C$, and $\delta^{18}O$, but also by significant variability in lithology, micropaleontology, mineralogy, and chemistry. The variability of these other parameters is useful for subdividing the critical part of the section into the following microstratigraphic intervals, going upward from shortly below the base of the clay marl unit (Fig. 10, Pa-I through Eo-IV):

***Paleocene-I* (*Pa-I*)**. A characteristic, 20-cm-thick, greenish-gray marl bed occurs below the clay marl unit and ends the underlying series of upper Paleocene reddish scaly marl facies (Fig. 11). This greenish-gray marl bed contains *Zoophycos* and *Chondrites*, and can be correlated to other sections in the Valbelluna, for example, Cicogna and Vena d'Oro Valley. The Pa-I bed does not contain any hematite (Fig. 10), which distinguishes it from adjacent layers. The $CaCO_3$ content varies from 35 to 55 wt%. Calcareous plankton and benthic foraminifera are diversified and well preserved. Taken together, these characteristics indicate that the Pa-I interval was deposited in well oxygenated waters above the lysocline.

***Paleocene-II* (*Pa-II*)**. The clay marl unit rests on a distinct, 1.5–2.0-cm-thick, dark gray marl interval (Fig. 11), in which $CaCO_3$ content has decreased to 28%. Increased carbonate dissolution is indicated also by sharply decreasing abundance of planktic foraminifera, where the planktic/benthic ratio is a mere 15% in comparison to the 95%–98% recorded in the underlying Pa-I interval. Benthic hyaline foraminifera are corroded and represent typical deep-water Paleocene fauna, e.g., *Gavelinella beccariiformis*, *Cibicidoides dayi, C. velascoensis*, *Neoflabelina semireticulata*, and *Pullenia coryelli*. The dissolution observed in Pa-II, immediately below the $\delta^{13}C$ negative excursion, presumably reflects the "dissolution burndown" front expected from an abrupt addition of massive quantities of $CO_2$ into the ocean (Dickens, 2000). Similar thin dissolution intervals immediately below the carbon isotope excursion have been reported from the South Atlantic and the Pacific Oceans (Thomas et al., 1999; Zachos et al., 2003; Colosimo et al., 2006).

***Black Clay***. A 0.2–0.3-cm-thick black clay, devoid of carbonate, is designated here as the base of the clay marl unit. A corresponding thin black clay layer has so far only been reported from the Shatsky Rise, where the layer was 0.1 cm thick (Bralower et al., 2002; Colosimo et al., 2006). The Forada black clay is characterized by a spike of biogenic barium (Fig. 10), a significant increase in organic carbon, and a complete absence of detrital mica. Mica occurs in all other (>100) investigated Forada samples and points to a brief interruption in the supply of coarse terrigenous materials, which makes it tenable to suggest that the black clay represents an episode of enhanced authigenic deposition. A scanning electron microscope study demonstrates the presence of ovoidal barite crystals at the boundary between the black clay and the underlying Pa-II interval (Fig. 11). The morphology of these crystals is similar to barite of organic origin (Paytan et al., 2002).

***Eocene-I* (*Eo-I*)**. The lowermost fossiliferous Eocene sediments consist of a 15–20-cm-thick, finely laminated greenish gray marl clay interval in which the average $CaCO_3$ content is ~15%. Planktic and benthic hyaline foraminifera are missing, and the only microfossils present are agglutinated foraminifera and a few strongly dissolved calcareous nannofossils. Deposition

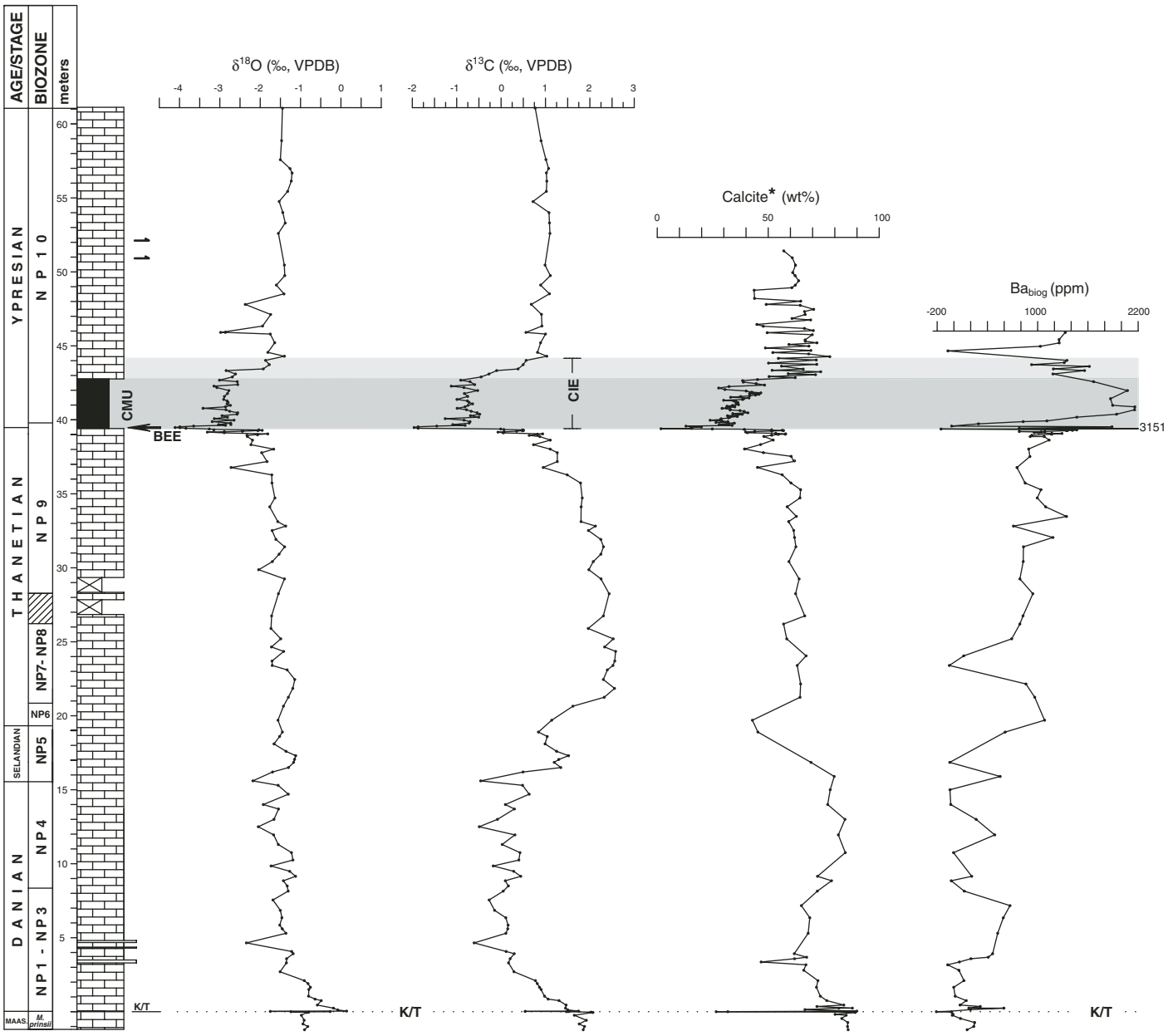


**Figure 9. Simplified columnar log, calcareous nannofossil biostratigraphy, stable isotopes stratigraphy ($\delta^{13}C$ and $\delta^{18}O$ measured on bulk sample), $CaCO_3$ and $Ba_{biog}$ of the entire late Maastrichtian–early Eocene Forada section. For detailed data on $Ba_{biog}$, see Figure 11. Shaded band denotes the interval enclosing the basal Eocene carbon isotope excursion (CIE). Calcite in the interval –122/+3205 cm was determined by recalculating chemical data (CaO and loss on ignition), whereas calcite in the interval +3252/+5142 cm was determined by coulometry. Analytical data are reported in Tables DR1, DR2, and DR3 (see text footnote 1). VPDB—Vienna Peedee belemnite standard; BEE—benthic extinction event; CMU—clay marl unit; K/T—Cretaceous-Tertiary boundary.**

presumably occurred close to a descending carbonate compensation depth (CCD), assuming that the CCD had briefly migrated above the Forada paleodepth during the accumulation of the underlying carbonate-free black clay. In Eo-I, $\delta^{13}C$ exhibits the most negative values, reworked Cretaceous calcareous nannofossils are common, and detrital quartz contents are high (Fig. 10). Strongly reduced, or lack of, bioturbation at the base of the carbon isotope excursion is recorded at other sections (Bralower et al., 1997), reflecting poorly ventilated to anoxic bottom waters but likely also strongly reduced and stressed benthic communities suffering from rapidly increasing bottom water temperatures and acidification (Zachos et al., 2005). The calcareous nannoplankton excursion taxa (*Discoaster anartios*, *D. araneus*, *Rhomboaster* spp.) enter the stratigraphic record at the top of Eo-I.

***Eocene-II* (*Eo-II*).** Calcareous nannofossil preservation improves and the calcareous nannofossil excursion taxa increase in abundance in the overlying, 20–25-cm-thick, greenish gray marl clay Eo-II interval, which has an average

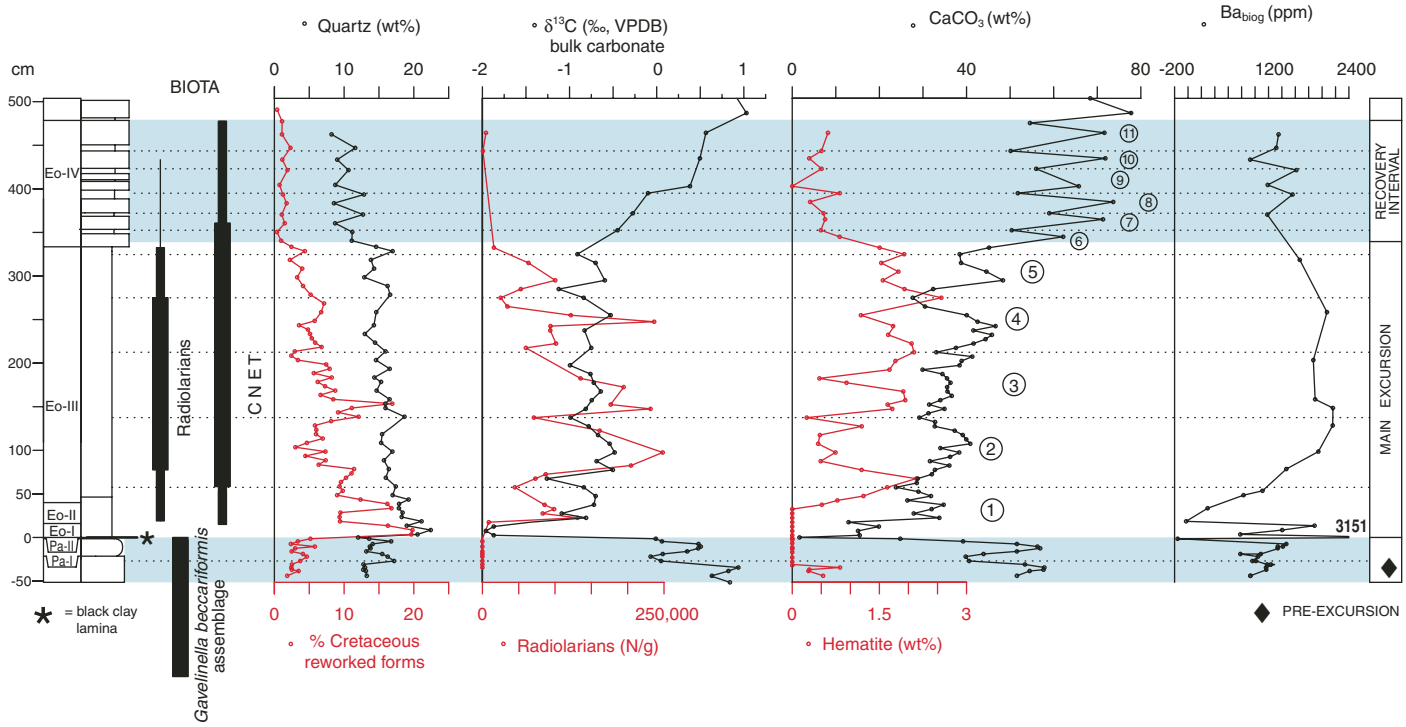


**Figure 10. Summary of the main biotic, mineralogical, and cyclostratigraphic features recognized across the Paleocene-Eocene boundary and in the clay marl unit (CMU) of the Forada section. Pa-I to Pa-II and Eo-I to Eo-IV denote the stratigraphic intervals discussed in the text. Analyses of radiolarians and foraminifera are based on the fraction >125 µm. CNET—calcareous nannoplankton excursion taxa; VPDB—Vienna Peedee belemnite standard.**

$CaCO_3$ content of 20%–30%. Common calcified radiolarians appear at the base of Eo-II. These forms thereafter remain at the top of the clay marl unit. Planktic foraminifera are still missing. An assemblage of rare and poorly preserved benthic hyaline foraminifera is present, although typical Paleocene forms of the *Gavelinella beccariiformis* assemblage (Thomas, 1998) are missing. The benthic foraminiferal extinction thus occurs in the 20 cm interval between the base of the black clay and the base of Eo-II, which is consistent with observations from deep-sea sites (e.g., Bralower et al., 2002; Lyle et al., 2002; Zachos et al., 2005). The preservation of micropaleontologic assemblages suggests persistent strong carbonate dissolution, still close to the CCD, albeit less severe than in the underlying Eo-I interval. The black clay together with the Eo-I and Eo-II intervals correlate with the carbonate dissolution interval (CDI) recorded in many deep-sea sites (Thomas, 1998), and in deep-water on-land sections such as the Trabakua Pass (Coccioni et al., 1994), Zumaya (Schmitz et al., 1997b, 2001), Alamedilla (Lu et al., 1996), and the Contessa Highway (Galeotti et al., 2000, 2004).

***Eocene-III* (*Eo-III*).** An ~290-cm-thick interval of mottled green and reddish marls with gradually increasing carbonate contents averaging

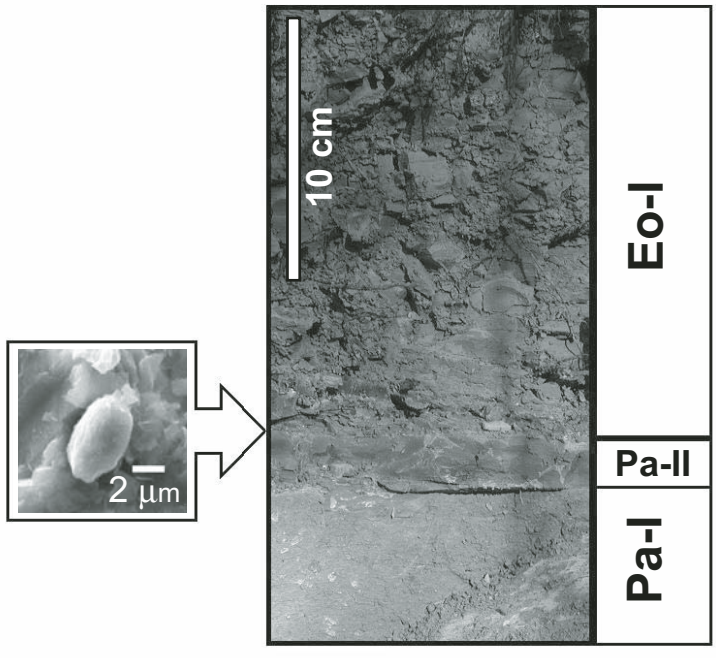


**Figure 11. Detail of the lowermost part of the CMU (clay marl unit) on the right bank of the Forada Creek. Inset: scanning electron micrograph of ovoidal barite crystal found in the partition between the "black clay" and the underlying Pa-II interval.**

around 35% makes up Eo-III (Fig. 10), which corresponds to the middle and upper part of the clay marl unit and the carbon isotope excursion main excursion. Eo-III is characterized by maximum values of hematite contents and the re-entry of planktic foraminifera at its base. Foraminiferal preservation improves rapidly upward in Eo-III, indicating a corresponding, rapidly descending CCD. But carbonate contents remain relatively low because of substantial terrigenous dilution. Radiolarians, calcareous nannofossil excursion taxa, and planktic foraminifera excursion taxa forms reach their maximum abundance.

***Eocene-IV* (*Eo-IV*).** Eo-IV consists of an ~145-cm-thick interval of reddish marl-limestone couplets, which represent the carbon isotope excursion recovery interval. Carbonate contents vary between 50% and 73% and are higher than in the uppermost Paleocene (Fig. 10). Radiolarians are virtually missing. The planktic foraminifera excursion taxa and calcareous nannofossil excursion taxa assemblages decrease in abundance upward and disappear at the very end of Eo-IV, at +4.60 m (Fig. 10), concomitant with the end of the carbon isotope excursion perturbation.

## Forada Mineralogy and Geochemistry across the Paleocene-Eocene Thermal Maximum

There are several reports indicating that mineralogical-geochemical parameters are sensitive to peculiar features of the Paleocene-Eocene thermal maximum, such as increased clay kaolinite (Robert and Kennett, 1994; Knox, 1998; Bolle and Adatte, 2001; Thiry, 2000; Schmitz et al., 2001), reduced ventilation in different oceanographic settings (e.g., Thomas, 1998; Kaiho et al., 1996; Kelly et al., 1996; Bralower et al., 1997; Speijer et al., 1997; Katz et al., 1999; Speijer and Wagner, 2002; Gavrilov et al., 2003), increased input of nutrients intensifying the biological pump (Bains et al., 2000; Zachos and Dickens, 2000), and addition of light $CO_2$ to the carbon cycle. All these parameters have been measured, and their significance is discussed below.

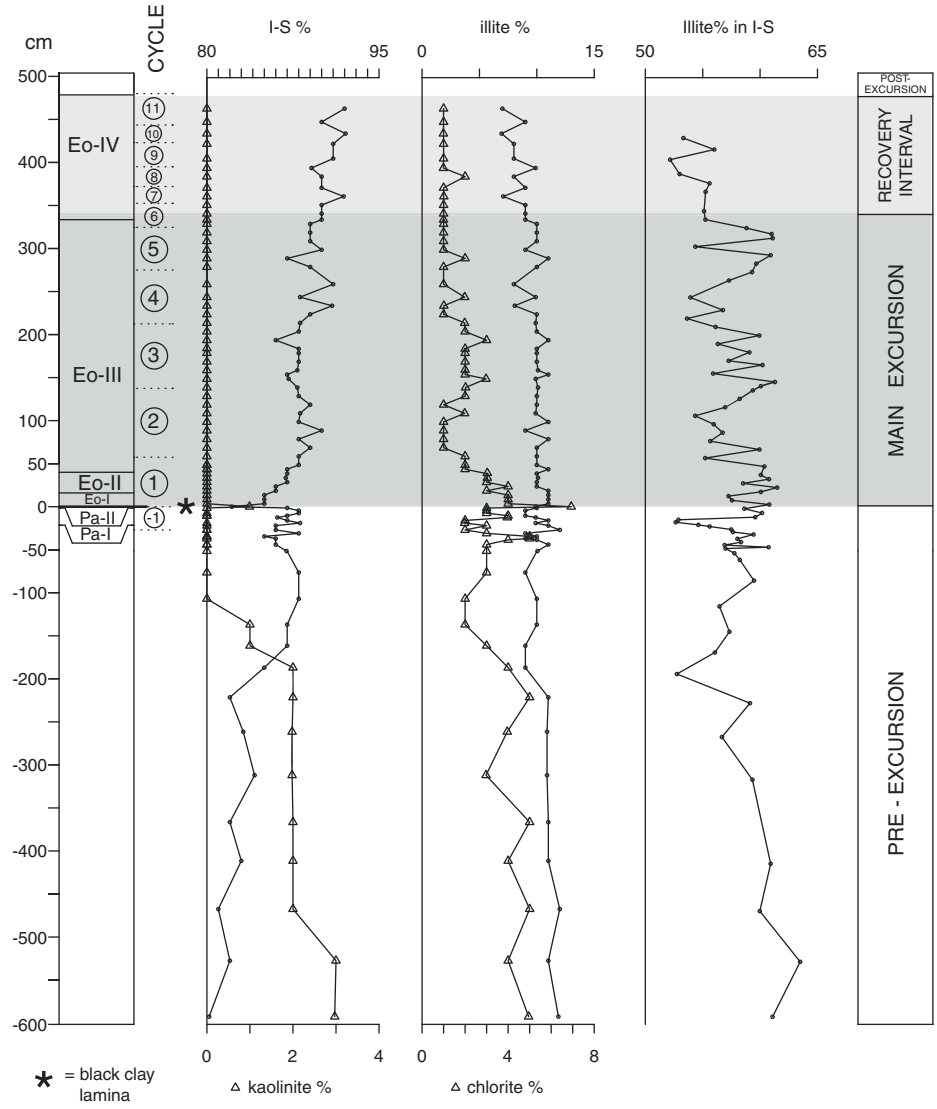


**Figure 12. Clay mineral assemblage in the late Paleocene and basal Eocene of the Forada section. The illite component of illite-smectite mixed layer is also reported (illite% in I-S). The clay mineral (<2 μm) variations across the Paleocene-Eocene thermal maximum are controlled by the long-term decrease of I-S upward, coupled with decrease of chlorite + illite. Also the content of illite in I-S varies from base to top, but with rather scattered values in the central part of the section. The kaolinite anomaly at the Paleocene-Eocene boundary reported by some authors (see text) is hardly detectable in the Forada section because kaolinite is at trace levels at the base of the section and is undetectable in the upper part.**

## Clay Minerals

Forada's clay mineral assemblages (Fig. 12) are strongly dominated by illite-smectite mixed-layers minerals (I-S), with random stacking order and rather low illite component (~50–60% illite), which suggests both that Forada belongs to the early diagenetic zone of Merriman and Peacord (1999) and that burial diagenesis has not affected the pristine mineralogy. The I-S gradually increases from the upper Paleocene and throughout the carbon isotope excursion. This trend is interrupted at the base of the clay marl unit, where I-S suddenly drops and remains lower than uppermost Paleocene in the Eo-I and Eo-II intervals. These I-S variations are coupled with an opposite trend of chlorite. Kaolinite is a minor component in the Paleocene and completely disappears ~1 m below the base of the clay marl unit, except for a single sample representing the black clay layer at the very base of the clay marl unit and carbon isotope excursion (Fig. 12). Thus, a source area of kaolinite was not available for erosion when the clay marl unit was deposited.

## Ventilation at Forada during the Paleocene-Eocene Thermal Maximum

Jones and Manning (1994) showed that V-Cr and Ni-Co ratios are indicators of paleo-oxygen levels. Ratios of these elements (Fig. 13A) vary

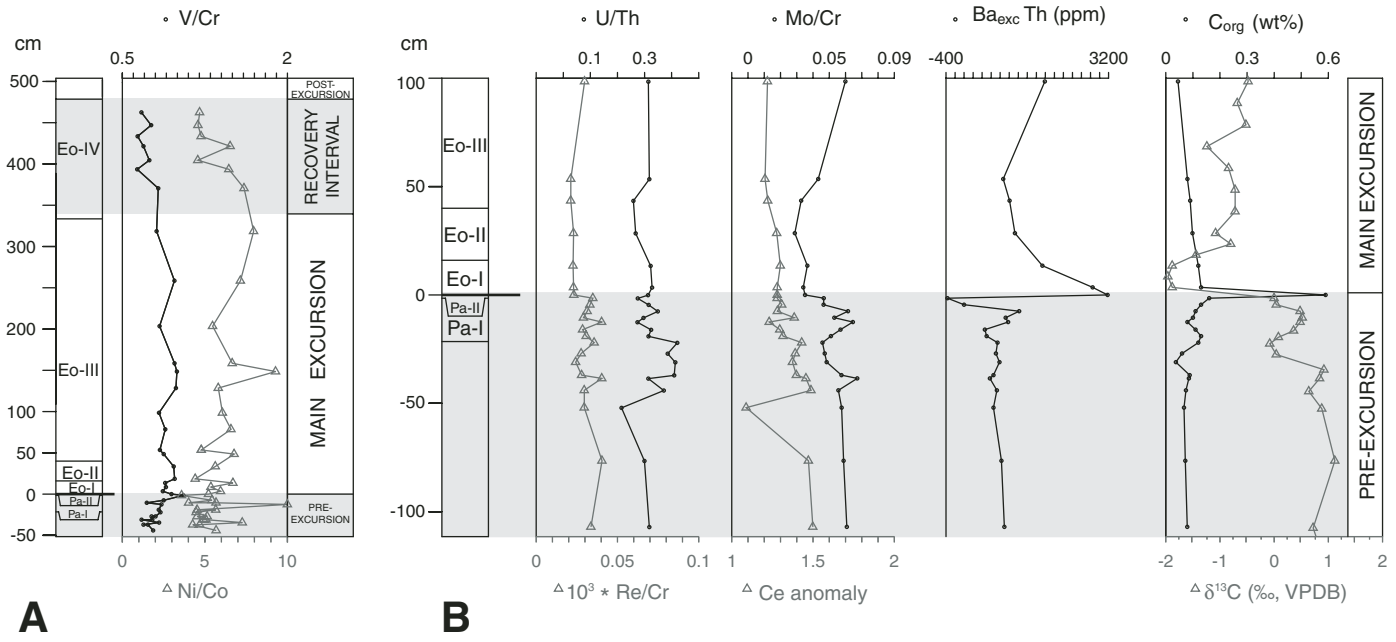


**Figure 13. (A) Geochemical indexes of bottom water oxygenation (V/Cr and Ni/Co) throughout the latest Paleocene–early Eocene of Forada section obtained from X-ray fluorescence (XRF) analyses. (B) Close-up of the 2 m across the Paleocene-Eocene boundary showing geochemical indexes of bottom water oxygenation (from instrumental neutron activation analysis), organic carbon content, and $\delta^{13}C$ bulk record. Ce anomaly = $3Ce_n/(2La_n + Nd_n)$; the notation Xn indicates the value of element X normalized to post-Archean American Shale (PAAS; Taylor and McLennan, 1985). $Ba_{exc}$ = barium excess (using Th as normalizing): $Ba_{sample} - (Th_{sample} \times Ba_{sample}/Th_{shale})$. VPDB—Vienna Peedee belemnite standard.**

within a narrow range, and significant differences are not observed between the well-oxygenated Paleocene sediments and the clay marl unit, indicating that Forada's bottom waters were well oxygenated. This is corroborated by intensive bioturbations, the abundance of benthic foraminifera, and the presence of oxidized minerals such as hematite.

A few trace elements (U, Mo, and Re) sensitive to redox conditions were measured in the critical 2 m interval across the black clay (Fig. 13B). Under reducing conditions, U is sorbed on preexisting solids or precipitates possibly as uraninite, while Mo is bound to sulfides or organic matter. The Re enrichment is perhaps the more reliable indicator of a suboxic or reducing environment because its detrital concentration is low and the authigenic accumulation is several orders of magnitude more than the crustal values (Morford and Emerson, 1999). These three elements (U, Mo, and Re), normalized to an index (Th or Cr in Fig. 13B), do not show any enrichment in the black clay or in the lower part of the Paleocene-Eocene thermal maximum (Eo-I, Eo-II, and basal Eo-III).

The so-called Ce anomaly has been considered as a redox proxy of bottom waters in Cretaceous sediments of the Belluno Basin (Bellanca et al., 1997), but no indication of low oxygenation is observed in Forada (Fig. 13B).

All considered redox indicators (V, U, Mo, Re normalized to a detrital index and Ni/Co ratio) concur in indicating that the Paleocene-Eocene thermal maximum at Forada was characterized by oxygenated bottom waters. The Paleocene-Eocene thermal maximum interval shows values similar to those in the underlying, well-oxygenated Paleocene sediments.

## Upper Paleocene and Paleocene-Eocene Thermal Maximum $Ba_{biog}$ Contents

The oxygenated condition during the carbon isotope excursion at Forada is a necessary condition for the preservation of biogenic barium accumulation (Paytan et al., 1993), which should register increased surface water productivity (Dymond et al., 1992). The productivity conditions are a debated point for significance in the Paleocene-Eocene thermal maximum in the global system (Thomas and Shackleton, 1996; Bains et al., 2000; Thomas, 2003; Bralower, 2002; Kelly, 2002; Stoll, 2004; Bralower et al., 2004).

Ovoid barite crystals, which have the size and morphology of marine barite (see Paytan et al., 2002, their Fig. 2), occur at the Pa-II to black clay transition (Fig. 11), and the black clay itself has the highest values of biogenic barium (3151 ppm). The black clay also preserves a single peak value of organic carbon (Fig. 13B). These features agree in indicating enhanced biogenic flux during the thin black interval. The absence of $Ba_{biog}$ in a single sample located 1.5 cm below the black clay (Fig. 10) probably represents dissolution caused by intrusion of reducing pore waters, in analogy with the carbonate dissolution observed in Pa-II. The $Ba_{biog}$ values vary strongly in Eo-I and Eo-II, but are relatively stable in Eo-III and Eo-IV (Fig. 10). The highest $Ba_{biog}$ values occur in the Paleocene-Eocene thermal maximum (Fig. 9), which is consistent with observations from other available marine Paleocene-Eocene thermal maximum intervals (Schmitz et al., 1997a; Bains et al., 2000; Faul and Paytan, 2005), whereas its meaning is still a matter of debate according to modeling approaches (Dickens et al., 2003).

## No Increase of Iridium at Forada

The hypothesis of a comet impact (Kent et al., 2003) is based on elevated abundance of magnetite nannoparticles in the carbon isotope excursion of the Bass River, at the base of the carbon isotope excursion, and of Ir enrichment in Zumaya and Goriška Brda (Schmitz et al.,

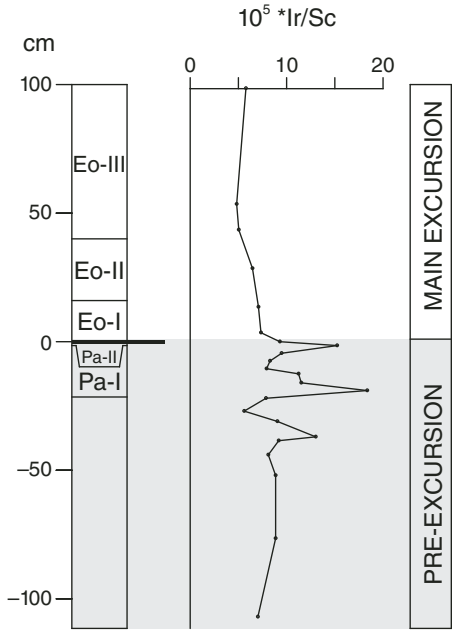


**Figure 14. Iridium-scandium ratio across the Paleocene-Eocene boundary at Forada section.**

1997b; Dolenec et al., 2000). In the latter section, the Ir anomaly is apparently more pronounced, even if the position of the Paleocene-Eocene boundary is poorly constrained (Dolenec et al., 2000). The Goriška Brda section and Forada are located ~120 km apart. Iridium contents have been determined in Forada in a 2 m interval across the onset of the Paleocene-Eocene thermal maximum. The concentration of Ir in the bulk rock ranges between 0.7 ppb and 3.6 ppb. However, the Ir distribution has been normalized to Sc, following a widely used procedure in order to avoid the diluting effects of carbonates and because Sc is not easily affected by postdepositional remobilization and is representative of detrital supply (Schmitz et al., 2004). The Ir/Sc (ppb/ppm) profile (Fig. 14) shows low values (below 0.1), with a few points between 0.1 and 0.2, but none of these higher values can be considered a significant anomaly. For comparison, the Ir/Sc ratio at the K-T boundary in the Forada is 2.9 (Fornaciari et al., 2007).

### Forada Paleodepth and Carbonate Data Support a Prodigious Acidification of the Global Ocean

A common feature of the Paleocene-Eocene thermal maximum observed in nearly all deep-water sections is the presence of a carbonate dissolution interval at its very base; this has been interpreted to represent a rapid shallowing of the CCD caused by acidification of the oceans (Dickens et al., 1997; Zachos et al., 2005). The exception is Ocean Drilling Program (ODP) Site 690 in the Southern Ocean (Kennett and Stott, 1991; Kelly et al., 2005). Dickens et al. (1997), assuming an input of ~1500–2000 Gt of carbon to the ocean-atmosphere system, predicted only a modest shallowing of the CCD of some 400 m. A much larger (>2000 m) shoaling of the CCD was inferred by Zachos et al. (2005), based on new core data from the Walvis Ridge in the South Atlantic. The basal 40–50 cm of sediments at the Forada Paleocene-Eocene thermal maximum were deposited below or close to the CCD, implying that estimates about Forada's paleodepth provide crucial information about the shoaling of the CCD in the central western Tethys as well as the degree of the global acidification of the ocean during the Paleocene-Eocene thermal maximum.

The Paleocene depositional depth of the Scaglia Rossa has been estimated to be on the order of ~1000 m (Poletti et al., 2004). Forada sediments host abundant representatives of the bathyal to abyssal Velasco benthic foraminiferal fauna (Berggren and Aubert, 1975), such as *Aragonia* spp., *Anomalinoides rubiginosus* s.s., *Cibicidoides dayi*, *Cibicidoides hyphalus*, *Cibicidoides velascoensis*, *Gaudryina pyramidata*, *Gyroidinoides globosus*, *Nuttallides truempyi*, *Gavelinella beccariiformis* s.s., *Quadratobuliminella pyramidalis,* as well as other taxa typical of middle bathyal to abyssal depths; e.g., *Bulimina trinitatensis*, *Gyroidinoides* spp., *Oridorsalis umbonatus*, *Paralabamina hillebrandti*, and *Spiroplectammina spectabilis*. Some of the most common species in Forada, such as *B. trinitatensis*, *N. truempyi*, and *G. beccariiformis* s.s., have upper depth limits of ~600 m (van Morkhoven et al., 1986; Alegret and Thomas, 2001; Alegret et al., 2003), whereas the lower bathyal-abyssal taxa, such as *Clavulinoides amorpha*, *Clavulinoides trilatera*, and abyssaminids (Kaminski et al., 1988; van Morkhoven et al., 1986), are rare. The Forada Paleocene-Eocene boundary sediments thus were deposited at paleodepths between ~600 m and 1000 m, but probably not deeper than 1500 m, according to the scheme of Van Morkhoven et al. (1986).

The fact that the CCD rose above the Forada paleodepth of ~1 km (± a few hundred meters) is consistent with observations from several ocean basins, including the Tethys (Thomas, 1998), that indicate a prodigious shallowing of the CCD and suggest that a much larger volume of $CO_2$ was added to the ocean-atmosphere system (Zachos et al., 2005) than the initial conservative estimate (Dickens et al., 1997).

### Chronology of the Paleocene-Eocene Thermal Maximum

When the $\delta^{13}C$ signature of the Paleocene-Eocene thermal maximum was first properly mapped, it was immediately recognized as a geologically brief event (Kennett and Stott, 1990). A Milankovitch-based cycle chronology was subsequently established for the carbon isotope excursion (Norris and Röhl, 1999; Röhl et al., 2000), despite the precision problems of the orbital solutions in the early Eocene (Pälike et al., 2004; Lourens et al., 2005). Röhl and colleagues concluded that the main carbon isotope excursion had a duration of ~90 k.y., whereas the duration of the recovery interval was 120–130 k.y. This age model was challenged by Cramer (2001), on the basis of a possible error caused by the number of cycles involved, and by Farley and Eltgroth (2003), on the basis of a $^3He$ chronology from ODP Site 690, a site used also by Röhl et al. (2000). Farley and Eltgroth proposed a duration for the main excursion of 80 k.y., but a strikingly lower (75%) duration of only 30 k.y. for the recovery interval. These two models thus agree fairly well on the duration of the main excursion, but disagree on the duration of the recovery interval.

The underlying causes of the occurrences of long series of repetitive alternating lithologies in marine sedimentary sections, such as between marls and limestones, are far from clear. Yet, pervasive deposition of lithological cycles in many Paleogene deep-sea environments has a demonstrably orbital pace (Weedon et al., 1997). Forada's Paleocene-Eocene thermal maximum interval includes a superbly well-developed lithological cyclicity in the controversial recovery interval, consisting of distinct marl-limestone couplets (Figs. 10 and 15). Geochemical and lithological cyclicity of the Paleocene-Eocene thermal maximum at ODP Sites 690 and 1051 is considered to represent precession cycles (Norris and Röhl, 1999; Röhl et al., 2000), a pacing that has been inferred also in marine on-land sections in eastern Valbelluna (Poletti et al., 2004) and Zumaya in northern Spain (Dinarès-Turell et al., 2002). Lourens et al. (2005) concluded that the Paleocene-Eocene thermal maximum event in the middle latitude South Atlantic exhibits orbital pacing in its preserved record of magnetic susceptibility and color reflectance. The early Eocene cyclicity of the middle latitude is hence assumed to represent precession cycles. This assumption is in agreement with calcareous nannofossil biostratigraphy. Specifically, at Forada, the last occurrence of *Fasciculithus* spp. occurs between the 16th and 17th cycles above the base of the carbon isotope excursion (Fig. 15; Agnini et al., 2005), and the event has

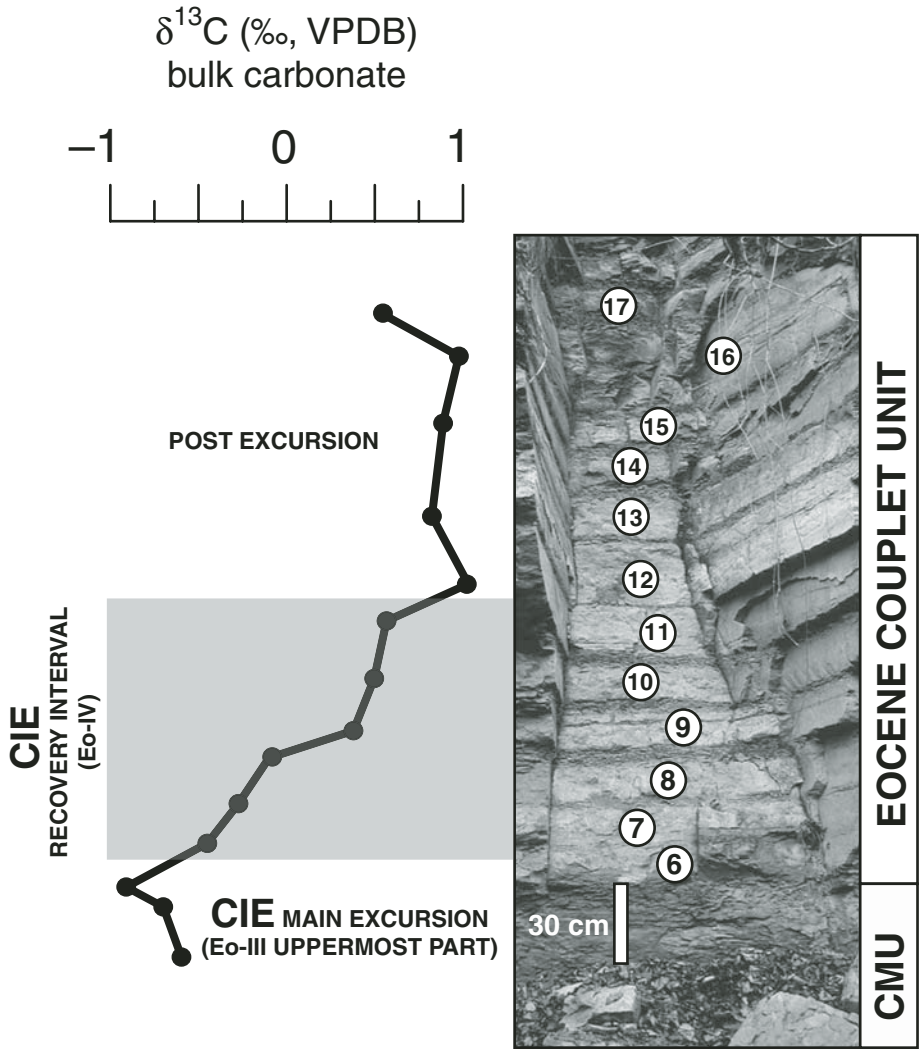


**Figure 15. $\delta^{13}C$ data of the recovery interval of the carbon isotope excursion (CIE) at Forada plotted against the well-developed marl-limestone couplets (Eocene couplet unit—ECU) overlying the clay marl unit (CMU). The last occurrence of calcareous nannofossil *Fasciculithus* spp. has been recorded between the 16th and 17th cycles above the base of the carbon isotope excursion. VPDB—Vienna Peedee belemnite standard.**

been estimated as having occurred 300 k.y. and 400 ± 10 k.y. above the carbon isotope excursion in the equatorial Pacific (Raffi et al., 2005) and in the southern Atlantic (Site 1262), respectively. This finding precludes anything other than precession Milankovian frequency as having paced the Forada cycles.

### Duration of the Carbon Isotope Excursion Main Excursion and the Recovery Interval

Visual lithological cycles are not apparent in Eo-I through Eo-III of the clay marl unit (Fig. 8), but several properties oscillate in fashions that have a cyclical character (Fig. 10). Calcified radiolarians occur only in the clay marl unit interval and show five distinct peaks in abundance. The $\delta^{13}C$ profile of the bulk sediment has a cyclical character and shows five discernible cycles, where heavier isotope values coincide with increasing radiolarian abundance. Heavier $\delta^{13}C$ values indicate increased productivity, which is consistent with increased radiolarian abundance. Hematite is absent in Eo-I and Eo-II, but shows four peaks in Eo-III separated by three distinct troughs. Finally, $CaCO_3$ shows a trend of progressively increasing contents throughout the clay marl unit, from an average of 16% in the four samples overlying the black clay to an average of 44% in the three uppermost clay marl unit samples. This trend of increasing carbonate, however, also shows cycles that, by and large, oscillate in concert with the carbon isotopes and that therefore presumably reflect variations in productivity.

Productivity variations expressed in radiolarian abundance, carbon isotopes, and carbonate contents suggest five cycles in Forada's clay marl unit. Above the hematite-free interval in the lower clay marl unit, hematite shows four cycles that roughly inversely correlate to carbonate.

Spectral analyses of sediment property cycles of the carbon isotope excursion in ODP Sites 690 and 1051 made Röhl et al. (2000) show that these cycles represent influence of precession. Forada's clay marl unit is thus here considered to yield five precessional cycles between the base of the clay marl unit–carbon isotope excursion and the base of the recovery interval (Eo-IV); this results in a main excursion duration of ~105 ± 10 k.y., if a span of 19–23 k.y./cycle is adopted (Berger, 1984).

Forada's main excursion (Fig. 10) is 3.39 ± 0.14 m long and is 2.7 times more expanded than the corresponding interval at ODP Site 690 (Kennett and Stott, 1990; Zachos et al., 1993), from which four precession cycles were recognized (Röhl et al., 2000).

Forada yields six well-developed marl-limestone couplets above the clay marl unit (Figs. 8, 10, and 15) in the carbon isotope excursion recovery interval (Eo-IV), which have a total duration of ~126 ± 12 k.y. if the identical age span for each cycle of Berger (1984) is adopted. Röhl et al. (2000) counted seven precession cycles from the corresponding recovery interval at ODP Site 690, which is one additional cycle in comparison to Forada, although cycle 6 was poorly developed (Röhl et al., 2000, their Fig. 3). The recovery interval is better resolved at Site 690 (2.4 m) than at Forada (1.4 m), although the six visual lithological couplets at Forada are unequivocally expressed in the carbonate record (Fig. 10). The entire carbon isotope excursion thus spans 11 complete precessional cycles at Forada and is not shorter than 209 k.y. and not longer than 253 k.y., with an average duration of 231 k.y.

## INCREASED PALEOCENE-EOCENE THERMAL MAXIMUM SEDIMENTATION RATES FROM TERRESTRIAL INPUT

A growing body of evidence supports the idea of an intensified hydrologic cycle during the Paleocene-Eocene thermal maximum because of the greenhouse-induced global warming (Dickens, 2000; Zachos and Dickens, 2000; Huber and Sloan, 2000; Bice and Marotzke, 2002; Dickens et al., 2003), which resulted in enhanced continental silicate weathering (Gibson et al., 1993; Robert and Kennett, 1994; Knox, 1998; Bolle

and Adatte, 2001; Schmitz et al., 2001; Ravizza et al., 2001; Crouch et al., 2003) and increased marine accumulation of clay-fraction kaolinite (Robert and Kennett, 1994; Knox, 1998; Bolle and Adatte, 2001; Thiry, 2000; Schmitz et al., 2001; Kelly et al., 2005).

Ravizza et al. (2001) demonstrated an anomalous continental osmium input to the oceans during the Paleocene-Eocene thermal maximum, which was interpreted to represent a 20%–30% higher global weathering flux that led to increased terrestrial fluxes and higher bulk sedimentation rates. Rates in Forada increase by nearly a factor of five when comparing the underlying upper Paleocene (NP9:7 m/m.y.) with the clay marl unit (33 m/m.y.), a rate increase compatible with data from northern Spain, where siliciclastic input appears to have increased 2–5 times in the Basque Basin (Schmitz et al., 2001), and bulk sediments appear to have increased 5–10 times in the Tremp Basin (Schmitz and Pujalte, 2003).

The increased abundance of radiolarians, reworked calcareous nannofossils, hematite, and quartz, together with a fivefold increase in sedimentation rate in the clay marl unit, points to a brief, albeit major, change in the continental weathering regime that resulted in hugely increased terrigenous input at Forada. The stratigraphic record of the near-continental Forada section is thus wholly consistent with the idea that continental silicate weathering accelerated during the Paleocene-Eocene thermal maximum through increased global temperatures and an enhanced hydrological cycle, permitting excess carbon to be permanently removed (Walker et al., 1981; Berner et al., 1983; Huber and Sloan, 1999; Zachos and Dickens, 2000).

## COMPARING THE MICROSTRATIGRAPHY OF THE $\delta^{13}C$ CARBON ISOTOPE EXCURSION RECORD AT FORADA WITH THAT OF ODP SITE 690 AND THE CONTINENTAL POLECAT SECTION

The larger-scale $\delta^{13}C$ stratigraphy measured on bulk sediment is generally similar in Forada and the corresponding record of ODP Site 690, although the structure of the signal differs in the fine-scale details (Fig. 16). A major difference between Forada and Site 690 is the stepped $\delta^{13}C$ shift in the latter record (Fig. 16). This step of ~10 cm in Site 690 has been the cause of much debate (Bains et al., 1999; Röhl et al., 2000; Bralower, 2002; Kelly, 2002; Thomas et al., 2002; Bralower et al., 2004; Kelly et al., 2005; Stoll, 2005). Surface-dwelling planktic foraminifera from Site 690 did not preserve this step,

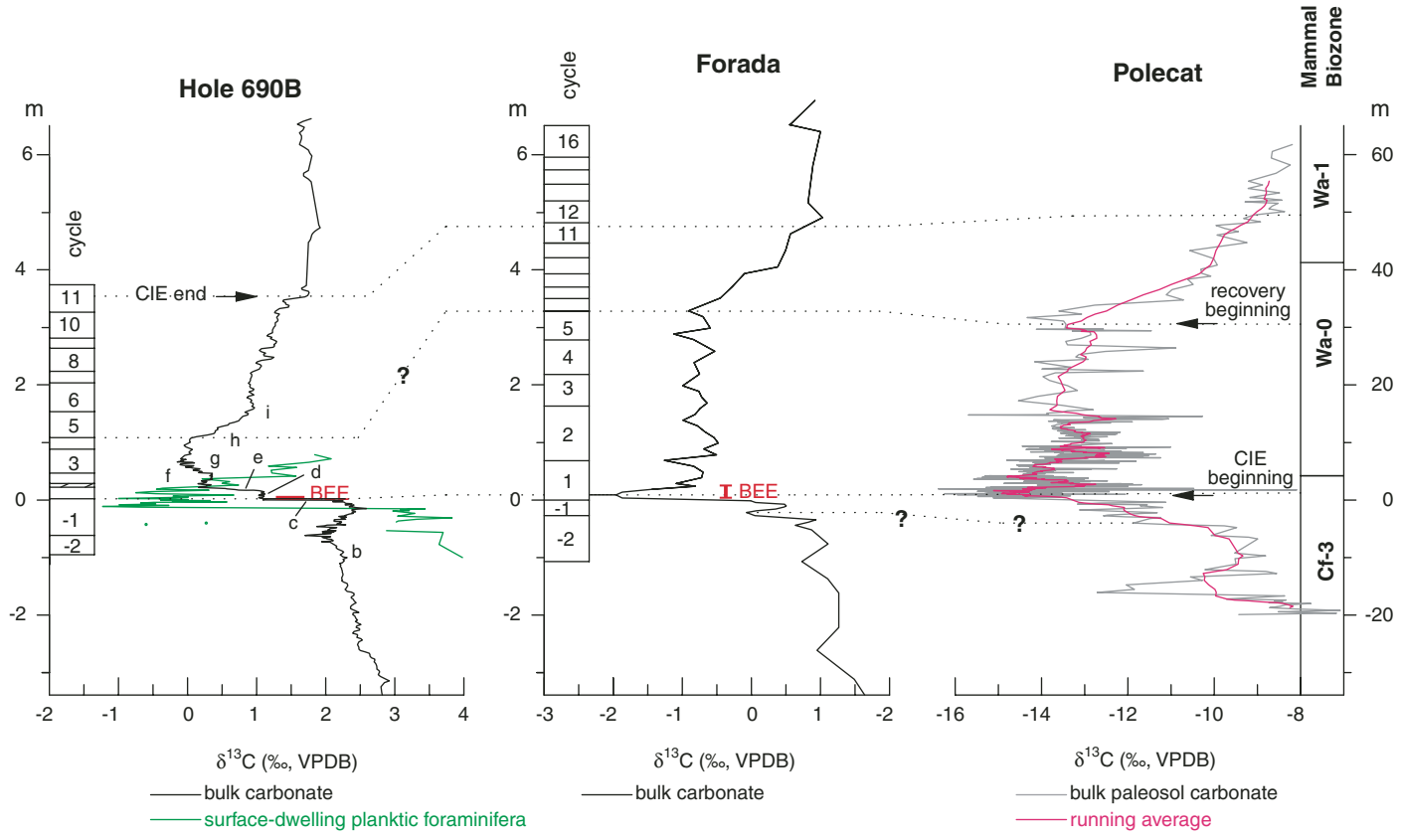


**Figure 16. The $\delta^{13}C$ bulk record through the Paleocene-Eocene thermal maximum interval at Forada section compared with $\delta^{13}C$ records of other marine and terrestrial Paleocene-Eocene thermal maximum reference sections. Terrestrial data derived from carbonate soil nodules from the Polecat Bench-South (northern Wyoming) are from Bains et al. (2003). Biozones based on mammalian faunas are from Gingerich (2003). The $\delta^{13}C$ record from Ocean Drilling Program (ODP) Site 690B (Weddell Sea), based on bulk carbonates and surface-dwelling planktic foraminifera, is from Bains et al. (1999) and Thomas et al. (2002), respectively. The labels b through i are used to denote events across the Paleocene-Eocene thermal maximum in Hole 690B as discussed in Bains et al. (1999). CIE—carbon isotope excursion; BEE—benthic extinction event; VPDB—Vienna Peedee belemnite standard.**

but show a single, sharp shift in $\delta^{13}C$ (Thomas et al., 2002) preceding the thermocline-dwelling planktic foraminifera and bulk sediment isotopic shift by 10 cm (≈10 k.y.). Stoll (2005) provided one of the most comprehensive discussions to date about the stepped $\delta^{13}C$ shift at Site 690 and the 10 k.y. lag between surface-dwelling foraminifera on the one hand and bulk carbonate and thermocline-dwelling foraminifera on the other. She concluded that the measured trends in the bulk sediment, chiefly represented by $\delta^{13}C$ preserved in calcareous nannofossils, are not artifacts but reflect genuine paleoceanographic signals, the causes of which remain uncertain.

It follows that differences in the detailed structure of the $\delta^{13}C$ record across the carbon isotope excursion may reflect preservation of regional paleoenvironmental characteristics or merely changing composition of the carbonate fraction. A nonstepped $\delta^{13}C$ shift of the carbon isotope excursion in the Northern Hemisphere thus does not necessarily imply the presence of a hiatus just because such a step occurs at a high-latitude Southern Hemisphere site.

Site 690, at a paleodepth of 1900 m (Thomas, 1998), shows an unusual, and unexplained, modest decline in carbonate content at the base of the Paleocene-Eocene thermal maximum (Kennett and Stott, 1991; Kelly et al., 2005) that is in stark contrast to several other deep-sea sites, where the basal Paleocene-Eocene thermal maximum is characterized by complete dissolution of carbonate (e.g., Bralower et al., 1997, 2002; Lyle et al., 2002; Zachos et al., 2005). Also, Forada shows a complete lack of carbonate in a single sample at the basal Paleocene-Eocene thermal maximum black clay and a general dominance of clays in the clay marl unit, but the clay marl unit of Forada represents a completely different depositional setting when compared to the carbonate-barren deep-sea sediments in the Atlantic and Pacific Oceans. Clay intervals in the deep-sea sites represent residual deposits in fully pelagic environments remote from terrestrial fluxes caused by carbonate dissolution, whereas the clay marl unit represents increased terrestrial fluxes in a near-continental, hemipelagic setting that resulted in increased sedimentation rates despite intense carbonate dissolution. The depositional setting of Forada thus argues against the presence of a hiatus at its base. Moreover, Forada's clay marl unit, or main $\delta^{13}C$ excursion, is one precessional cycle longer than any other known marine Paleocene-Eocene thermal maximum interval, implying that the stratigraphy of Forada also argues against a hiatus. Still, if a hiatus is present at Forada, and assuming that the main excursion interval has a duration of ~80 k.y. (Röhl et al., 2000), this would imply that Forada's apparent cycles in $\delta^{13}C$, as well as in the abundance of radiolarians, carbonate content, and hematite, do not carry an orbital pacing, which would reflect also on Sites 690 and 1051, where such a pacing has been implied using similar sediment properties.

An intriguing feature of the carbon isotope excursion at Forada is its similarity with a ten times more expanded continental $\delta^{13}C$ record from the corresponding time interval derived from soil nodule carbonates in the Polecat section in Wyoming (Bowen et al., 2001; Fig. 16). The main excursion interval in both records shows the most negative values at its very base, followed by a higher-frequency variability along a gently sloping return toward heavier values to the top of this interval. The transition to the recovery interval is sharp in both records.

Available data from the expanded main excursion interval at Forada, together with the fact that its $\delta^{13}C$ stratigraphy mimics that of the continental Polecat section, make it tenable to suggest that the carbon isotope excursion interval represents continuous deposition, that the nonstepped initial $\delta^{13}C$ excursion represents an indigenous signal, and that Forada preserves a $\delta^{13}C$ main excursion interval that is one of the most complete such intervals presently available from a marine setting.

### The Prelude, Mode, and Tempo of the Paleocene-Eocene Thermal Maximum

The environmental conditions preceding the Paleocene-Eocene thermal maximum as well as the mode and tempo of the addition of $CO_2$ to the exogenic carbon system are not yet solved. The conditions preceding the Paleocene-Eocene thermal maximum have been barely considered in high-resolution studies despite evidence of instabilities in temperature (Thomas et al., 2002), salinity (Tripati and Elderfield, 2004), and in biotic communities (Bralower, 2002; Stoll, 2005) preceding the major carbon isotope shift. Bains et al. (1999) and Dickens (2001) interpreted the stepped pattern of the bulk sediment excursion at Site 690 to be related to pulsed additions of light carbon to the exogenic carbon system.

The stratigraphy of the Forada section and the Polecat continental record (Fig. 16) would suggest that there was a major catastrophic release of light carbon at the onset of the Paleocene-Eocene thermal maximum. This event is recorded in the sharp lithologic contact at the base of the clay marl unit, which is interpreted to have been caused by a sudden and prodigious shallowing of the CCD, driven by acidification of the ocean below the thermocline zone (Zachos et al., 2005). This implies that the stepped carbon isotope excursion at Site 690 in the Southern Ocean presumably reflects regional paleoceanographic conditions. Site 690 is also unusual in being the only existing deep-sea site in which carbonate is largely preserved across the initial carbon isotope excursion.

A characteristic feature in most other marine sections is the enhanced dissolution at the base of the Paleocene-Eocene thermal maximum. At the paleodepth of Forada, the most intense dissolution lasted a few thousand years, <0.5 precession cycle (Fig. 10). At the transition between the first and the second precession cycles (Fig. 10), some 20 k.y. after the onset of the Paleocene-Eocene thermal maximum, the CCD deepened enough to permit preservation of planktic foraminifera and carbonate deposition (Eo-III). However, the carbon system remained perturbed throughout the remainder of the main excursion (Eo-III), ~80 k.y., in the ocean (Forada) as well as in the atmosphere (Polecat). The silicate and biological pumps were at work during Eo-III, which resulted in a minor, gently sloping, return toward heavier $\delta^{13}C$ values (≈0.25‰ at Forada; Fig. 10).

The transition to the recovery interval is sharp in terms of lithologic change as well as in $\delta^{13}C$. Forada suggests that the silicate pump and continental weathering occurred throughout the main excursion. One simple way to explain the length of the main excursion and the sharpness of the transition between the main excursion and the recovery interval is that the source of the light $CO_2$ ceased at the top of the clay marl unit (approximately the end of the main excursion). Dickens (2001) noted that it is highly unlikely that the Paleocene-Eocene thermal maximum was caused by a single blast of carbon. The base of the recovery interval marks the time when light carbon ceased to be added to the ocean-atmosphere system, which permitted the carbonate deposition to fully resume at Forada, resulting in the formation of limestone-marl couplets. The transition also marks the beginning of the gradual disappearance of radiolarians, calcareous nannofossil excursion taxa, and planktic foraminifera excursion taxa, and the recovery of $\delta^{13}C$ values to pre-excursion stable values. It took ~126 ± 12 k.y. for the system to be completely restored through removal of the excess of light carbon. This duration of the recovery is in agreement with modeling (e.g., Dickens et al., 1997; Dickens, 2001; Zachos et al., 2005).

## SUMMARY AND CONCLUSIONS

Calcareous nannofossil biostratigraphies from the previously undescribed Ardo, Cicogna, and Forada sections in the Valbelluna region of the Venetian pre-Alps (NE Italy) demonstrate the preservation of nearly continuous deposition of Upper Cretaceous through lower Eocene

hemipelagic to pelagic sediments. A composite record of cyclically organized limestone-marl couplets can be reconstructed by splicing sections in the river cuts, which exhibit condensed lower Paleocene (NP1–middle NP4) but relatively expanded middle and upper Paleocene (middle NP 4–middle NP9), and lowermost Eocene (upper NP 9–NP 10) sections >100 m thick. A prominent feature in these Valbelluna sections is the 3–4-m-thick lithologic anomaly, consisting of greenish-reddish clay and marls (clay marl unit), that sharply interrupts the underlying and overlying limestone-marl couplets. Paleocene benthic foraminifera disappear at the base of the clay marl unit, although the exact position of the extinction is blurred by carbonate dissolution in the basal clay marl unit. Calcareous nannofossil biostratigraphy also indicates that the base of the clay marl unit coincides with the Paleocene-Eocene boundary. Moreover, the clay marl unit corresponds to the main interval of the carbon isotope excursion of the Paleocene-Eocene thermal maximum event. Immediately above the clay marl unit, carbonate sedimentation resumes with the deposition of distinct marl-limestone couplets.

Stable isotope analysis of bulk sediment samples from the Forada section closely reproduces the $\delta^{13}C$ Paleocene global trends, suggesting that the consolidated sediments of the Valbelluna sections by and large have preserved an indigenous carbon isotope record. A transient and nonstepped negative shift of 2.35‰ in $\delta^{13}C$ occurs over a 12.5 cm interval across the base of the 3.3-m-thick clay marl unit of Forada. The slightly heavier $\delta^{13}C$ values in the clay marl unit, in comparison to bulk sediment values from the corresponding interval in several open ocean sites, were probably caused by reworking of isotopically heavier Cretaceous calcareous nannofossils in Forada, which represent up to 20% of the total assemblage in the clay marl unit and which likely subdued the bulk sediment amplitude of the initial excursion in Forada

A single sample at the very base of the clay marl unit lacks calcium carbonate. Preservation of biogenic carbonate progressively increases upward in the clay marl unit, which is consistent with a scenario in which the CCD rapidly and briefly ascended above the depositional depth of the Forada sediments, estimated to be ~1000 ± 500 m, followed by a slower, successive deepening throughout the clay marl unit. The lowermost ~40 cm of the clay marl unit correlate with the "carbonate dissolution interval" in several deep-sea sites and in deep-water on-land sections such as the Trabakua Pass, Zumaya, Alamedilla, and the Contessa Highway. These records of carbonate preservation strongly support the idea of a prodigiously abrupt and rapid acidification of the oceans at the base of the carbon isotope excursion. The resulting extensive carbonate dissolution may be considered to represent the most consistent, in terms of isochrony, expression of the onset of the carbon isotope excursion event. The trigger of the event and the source of the huge amount of light $CO_2$ remain elusive. Results from Forada, however, do not preserve an iridium anomaly that would support an impact hypothesis.

A series of geochemical proxies for redox conditions was measured in Forada, which all concur in indicating that deposition occurred in oxygenated waters below and above the clay marl unit, and that such conditions endured throughout this interval except for its <0.3-cm-thick basal black clay layer. If methane was the source of the light carbon, evidently it had been delivered to the atmosphere from where it entered the oceans successively, as has been previously suggested. Preservation of ovoid biogenic barium crystals together with a peak value of organic carbon in the black clay layer indicate a brief episode of enhanced biogenic productivity.

Concentrations of hematite and biogenic carbonate, abundance of radiolarians, and the $\delta^{13}C$ record, all show cyclical variations in the clay marl unit. Taken together, there are five such cycles preserved in the clay marl unit at Forada, which are interpreted as precessional cycles. The total duration of this interval is thus 105 ± 10 k.y. if a span of 19–23 k.y./cycle is adopted. The main excursion interval at Forada is thus estimated to have a duration that is ~5%–30% longer compared to most previously published estimates, presumably reflecting the more expanded, and thus much better resolved, main excursion interval (clay marl unit) at Forada compared to most other carbon isotope excursion intervals. The overlying recovery interval consists of six limestone-marl couples, which also are interpreted to represent precessional cyclicity, and thus have a total duration of 126 ± 12 k.y. if the identical age span for each cycle is adopted. The recovery interval is not better resolved in Forada, but it has a more clear lithological expression in its distinct limestone-marl couplets when compared to most other recovery intervals. The duration of the recovery interval is in agreement with age models based on cycle counts of this interval in open ocean sites, but disagrees with an age model based on $^3He$ chronology. Given these limits, it follows that the entire carbon isotope excursion event in Forada is not shorter than 209 k.y. and not longer than 253 k.y., with an average duration of 231 k.y.

The mode and tempo of the light carbon added to the exogenic system and its subsequent removal across the carbon isotope excursion event are still poorly understood. Presumably, complete open ocean sites have yielded $\delta^{13}C$ profiles across the basal carbon isotope excursion that show a stepped pattern, with the lightest values attained in the middle of the main excursion. The profile at Forada shows a major lightening at the very base of the carbon isotope excursion, followed by relatively stable values, although cyclic, for most of the main excursion interval, followed by a rapid transition to pre-excursion values in the recovery interval. The nonstepped main excursion of the Forada with respect to some open ocean successions may of course originate from vagaries of the $\delta^{13}C$ signal in bulk carbonates or by discontinuity in sedimentation. The hemipelagic, near-continental depositional setting of Forada and the sharply increasing sedimentation rates at the onset and during the main excursion, however, strongly argue for continuous rather than interrupted deposition.

The $\delta^{13}C$ profile at Forada is strikingly similar to that observed in the continental Polecat section, suggesting a common response in the ocean-atmosphere system driven by the evolution of the global carbon system. Following the initial blast of light carbon into the ocean-atmosphere system at the base of the carbon isotope excursion, $\delta^{13}C$ values remained light over at least four precessional cycles, notwithstanding the buffering effect of the massive carbonate dissolution observed globally in virtually all parts of the oceans from the abyss to upper bathyal depths. Apparently light carbon continued to be added to the ocean-atmosphere system throughout the main excursion interval, even if the CCD never became as shallow as during the initial blast. The transition between the main excursion and the recovery interval is so sharp at Forada that it is best explained by a scenario in which the source of the light $CO_2$ was exhausted; that is, light carbon ceased to be added and was removed from the ocean-atmosphere system in a time span corresponding to approximately six precessional cycles.

Both the biological and silicate pumps have been invoked to explain the removal of the light carbon from the exogenic system. The efficiency of the biological pump during the carbon isotope excursion is a much debated issue. Prevailing scenarios envisage conditions of enhanced productivity in shelf settings and conditions of oligotrophy in the open oceans. The Forada section appears to be characterized by eutrophic conditions, considering the strongly increased terrigenous input and the abundance and preservation of radiolarians, but this section adds little to the existing debate on open ocean conditions because of its near-continental hemipelagic setting. Nevertheless, results from Forada indicate that the silicate pump must have played an important role as a potential sink of

the enormous mass (>>2000 Gt) of light carbon that is implied by the large-scale acidification and shoaling of the CCD at the onset of the carbon isotope excursion. The Forada chronology indicates an astonishing fivefold increase in sedimentation rate during the main excursion of the carbon isotope excursion, in spite of intense carbonate dissolution. Open ocean sites, in contrast, are typically characterized by a drastic decrease in sedimentation rate during the main excursion interval caused by carbonate dissolution, chiefly preserving a clayey residue. The increase in sedimentation rates at Forada, although not constrained in terms of absolute flux, was caused by increased terrigenous input from surrounding continents, which, in turn, presumably was caused by an intensified hydrological cycle and its resulting enhanced weathering and erosion in the carbon isotope excursion super-greenhouse world. The sharp transition to the recovery interval, characterized by resumed carbonate deposition and a marked shift toward heavier $\delta^{13}C$, suggests that the silicate pump and the continental weathering, the direct cause of the enhanced terrigenous flux to Forada during the main excursion interval, stopped abruptly.

It has been previously pointed out that a more comprehensive understanding of the carbon isotope excursion event requires study of numerous high-quality records from a range of different latitudes and water depths. The Forada section provides one such much needed record, and it adds an important piece to that puzzle, representing a middle latitude central western Tethys setting in middle to lower bathyal depths.

## ACKNOWLEDGMENTS

The work was supported by the financial support from COFIN Murst 2001 "Cretaceous to Paleogene Extreme Climates and Transient Climatic Events as Documented in Ocean Drilling Program (ODP) and On Land Pelagic Successions," coordinated by I. Premoli Silva (national) and D. Rio (Padova). Financial support provided by the University of Padova to E. Fornaciari, and by Stockholm University to J. Backman is much appreciated. We thank Elisabeth Burton, Deborah Thomas, and Heiko Pälike for the careful reviews that helped improve this work. Discussion with "Ulla" Röhl in the field has greatly improved our understanding of the Paleocene-Eocene thermal maximum. D. Rio is grateful to Jerry Dickens and Henk Brinkhuis for discussions about the Forada section during a memorable cruise to the Arctic Ocean. Thanks are due to Lorenzo Franceschin for processing samples for micropaleontological analyses.

## REFERENCES CITED

Agnini, C., Fornaciari, E., Giusberti, L., Backman, J., Capraro, L., Grandesso, P., Luciani, V., Muttoni, G., Rio, D., and Tateo, F., 2005, The early Paleogene of the Valbelluna (Venetian Southern Alps), *in* Field trip Guidebook Ocean Drilling Program (ODP) Leg 208 Post-Cruise Meeting: Padova, Cooperativa Libraria Editrice Università di Padova (CLEUP), 32 p.

Agnini, C., Muttoni, G., Kent, D.V., and Rio, D., 2006, Eocene biostratigraphy and magnetic stratigraphy from Possagno, Italy: The calcareous nannofossil response to climate variability: Earth and Planetary Science Letters, v. 241, p. 815–830, doi: 10.1016/j.epsl.2005.11.005.

Alegret, L., and Thomas, E., 2001, Upper Cretaceous and lower Paleogene benthic foraminifera from northeastern Mexico: Micropaleontology, v. 47, p. 269–316, doi: 10.2113/47.4.269.

Alegret, L., Molina, E., and Thomas, E., 2003, Benthic foraminiferal turnover across the Cretaceous/Paleogene boundary at Agost (southeastern Spain): Marine Micropaleontology, v. 48, p. 251–279.

Alegret, L., Ortiz, S., Arenillas, I., and Molina, E., 2005, Paleoenvironmental turnover across the Paleocene/Eocene boundary at the stratotype section in Dababiya (Egypt) based on benthic foraminifera: Terra Nova, v. 17, p. 526–536, doi: 10.1111/j.1365-3121.2005.00645.x.

Arenillas, I., Molina, E., and Schmitz, B., 1999, Planktic foraminiferal and $\delta^{13}C$ isotopic changes across the Paleocene/Eocene boundary at Possagno (Italy): International Journal of Earth Sciences, v. 88, p. 352–364, doi: 10.1007/s005310050270.

Aubry, M.-P., Ouda, K., Dupuis, C., Van Couvering, J.A., and the Members of the Working Group on the Paleocene/Eocene Boundary, 2002, Proposal: Global Standard Stratotype Section and Point (GSSP) at the Dababiya section (Egypt) for the base of the Eocene Series: International Subcommission on Paleogene Stratigraphy, Internal Report, 58 p.

Baceta, J.I., Pujalte, V., Dinarès-Turell, J., Payros, A., Orue-Extebarria, X., and Bernaola, G., 2000, The Paleocene/Eocene boundary interval in the Zumaia section (Gipuzkoa, Basque Basin): Magnetostratigraphy and high-resolution lithostratigraphy: Revista de la Sociedad Geologica de España, v. 13, p. 375–391.

Backman, J., and Shackleton, N.J., 1983, Quantitative biochronology of Pliocene and early Pleistocene calcareous nannoplankton from the Atlantic, Indian and Pacific Oceans: Marine Micropaleontology, v. 8, p. 141–170, doi: 10.1016/0377-8398(83)90009-9.

Bains, S., Corfield, R.M., and Norris, R.D., 1999, Mechanisms of climate warming at the end of the Paleocene: Science, v. 285, p. 724–727, doi: 10.1126/science.285.5428.724.

Bains, S., Norris, R.D., Corfield, R.M., and Faul, K.L., 2000, Termination of global warmth at the Palaeocene/Eocene boundary through productivity feedback: Nature, v. 407, p. 171–174, doi: 10.1038/35025035.

Bains, S., Norris, R.D., Corfield, R.M., Bowen, G.J., Gingerich, P.D., and Koch, P.L., 2003, Marine-terrestrial linkages at the Paleocene-Eocene boundary, *in* Wing, S.L., et al., eds., Causes and Consequences of Globally Warm Climates in the Early Paleogene: Geological Society of America Special Paper 369, p. 11–23.

Barahona, E., 1974, Arcillas de ladrillería de la provincia de Granada: Evaluación de algunos ensayos de materias primas [Ph.D. thesis]: Granada, Spain, University of Granada, 398 p.

Bellanca, A., Masetti, D., and Neri, R., 1997, Rare earth elements in limestone/marlstone couplets from the Albian-Cenomanian Cismon section (Venetian region, northern Italy): Assessing REE sensitivity to environmental changes: Chemical Geology, v. 141, p. 141–152, doi: 10.1016/S0009-2541(97)00058-2.

Berger, A., 1984, Accuracy and frequency stability of the Earth's orbital elements during the Quaternary, *in* Berger, A., Imbrie, J., Hays, J., Kukla, G., and Salzman, B., eds., Milankovitch and Climate: North Atlantic Treaty Organization (NATO) ASI Series C, v. 126, Part I, p. 3–39.

Berggren, W.A., and Aubert, J., 1975, Paleocene benthonic foraminiferal biostratigraphy, paleobiogeography and paleoecology of Atlantic-Tethyan regions: Midway-type fauna: Palaeogeography, Palaeoclimatology, Palaeoecology, v. 18, p. 73–192, doi: 10.1016/0031-0182(75)90025-5.

Berggren, W.A., Lucas, S., and Aubry, M.-P., 1998, Late Paleocene–early Eocene climatic and biotic evolution: An overview, *in* Aubry, M.-P., et al., eds., Late Paleocene–Early Eocene Climatic and Biotic Events in the Marine and Terrestrial Records: New York, Columbia University Press, p. 1–17.

Berner, R.A., Lasaga, A.C., and Garrels, R.M., 1983, The carbonate–silicate geochemical cycle and its effect on atmospheric carbon dioxide: American Journal of Science, v. 283, p. 641–683.

Bernoulli, D., and Jenkyns, H.C., 1974, Alpine, Mediterranean, and Central Atlantic Mesozoic facies in relation to the early evolution of the Tethys, *in* Dott, R.H., Jr., and Shaver, R.H., eds., Modern and Ancient Geosynclinal Sedimentation: Society for Sedimentary Geology (SEPM) Special Publication, v. 19, p. 19–160.

Bernoulli, D., Caron, C., Homewood, P., Kalin, O., and Van Stuijvenberg, J., 1979, Evolution of continental margins in the Alps: Schweizerische Mineralogische und Petrographische Mitteilungen, v. 59, p. 165–170.

Bice, K.L., and Marotzke, J., 2002, Could changing ocean circulation have destabilized methane hydrate at the Palaeocene/Eocene boundary?: Paleoceanography, v. 17, p. 1018, doi: 10.1029/2001PA000678.

Biscaye, P.E., 1965, Mineralogy and sedimentation of recent deep-sea clay in the Atlantic Ocean and adjacent seas and oceans: Geological Society of America Bulletin, v. 76, p. 803–832.

Bolle, M.-P., and Adatte, T., 2001, Palaeocene–early Eocene climatic evolution in the Tethyan realm: Clay mineral evidence: Clay Minerals, v. 36, p. 249–261, doi: 10.1180/000985501750177979.

Bosellini, A., 1989, Dynamics of Tethyan carbonate platform, *in* Crevello, P.D., et al., eds., Controls on Carbonate Platform and Basin Platform: Society for Sedimentary Geology (SEPM) Special Publication 44, p. 3–13.

Bowen, G.J., Koch, P.L., Gingerich, P.D., Norris, R.D., Bains, S., and Corfield, R.M., 2001, Refined isotope stratigraphy across the continental Paleocene-Eocene boundary on Polecat Bench in the northern Bighorn Basin, *in* Gingerich, P.D., ed., Paleocene-Eocene Stratigraphy and Biotic Change in the Bighorn and Clarks Fork Basins, Wyoming: University of Michigan Papers on Paleontology, v. 33, p. 73–88.

Bralower, T.J., 2002, Evidence of surface water oligotrophy during the Paleocene-Eocene thermal maximum: Nannofossil assemblage data from Ocean Drilling Program Site 690, Maud Rise, Weddell Sea: Paleoceanography, v. 17, doi: 1029/2001PA000662.

Bralower, T.J., Zachos, J.C., Thomas, E., Parrow, M., Paull, C.K., Kelly, D.C., Premoli Silva, I., Sliter, W.V., and Lohmann, K.C., 1995, Late Paleocene to Eocene paleoceanography of the equatorial Pacific Ocean: Stable isotopes recorded at Ocean Drilling Program Site 865: Allison Guyot: Paleoceanography, v. 10, p. 841–865, doi: 10.1029/95PA01143.

Bralower, T.J., Thomas, D.J., Zachos, J.C., Hirschmann, M.M., Röhl, U., Sigurdsson, H., Thomas, E., and Whitney, D.L., 1997, High-resolution records of the late Paleocene thermal maximum and circum-Caribbean volcanism: Is there a causal link?: Geology, v. 25, p. 963–966, doi: 10.1130/0091-7613(1997)025<0963:HRROTL>2.3.CO;2.

Bralower, T.J., Premoli Silva, I., Malone, M., et al., 2002, Proceedings of the Ocean Drilling Program, Initial reports, Volume 198, http://www-odp.tamu.edu/publications/198_IR/198ir.htm (accessed February 2006).

Bralower, T.J., Kelly, D.C., and Thomas, D.J., 2004, Comment on "Coccolith Sr/Ca records of productivity during the Paleocene-Eocene thermal maximum from the Weddell Sea" by Heather M. Stoll and Santo Bains: Paleoceanography, v. 19, p. PA1014, doi: 10.1029/2003PA000953.

Canudo, J.I., Keller, G., Molina, E., and Ortiz, N., 1995, Planktic foraminiferal turnover and $\delta^{13}C$ isotopes across the Paleocene-Eocene transition at Caravaca and Zumaya, Spain: Palaeogeography, Palaeoclimatology, Palaeoecology, v. 114, p. 75–100, doi: 10.1016/0031-0182(95)00073-U.

Cati, A., Sartorio, D., and Venturini, S., 1989, Carbonate Platforms in the Subsurface of the Northern Adriatic Area: Memorie della Società Geologica Italiana, v. 40, p. 295–308.

Channell, J.E.T., and Medizza, F., 1981, Upper Cretaceous and Palaeogene magnetic stratigraphy and biostratigraphy from the Venetian (southern) Alps: Earth and Planetary Science Letters, v. 55, p. 419–432, doi: 10.1016/0012-821X(81)90169-2.

Channell, J.E.T., D'Argenio, B., and Horvath, F., 1979, Adria, the African promontory in Mesozoic Mediterranean palaeogeography: Earth-Science Reviews, v. 15, p. 213–292, doi: 10.1016/0012-8252(79)90083-7.

Channell, J.E.T., Doglioni, C., and Stoner, J.S., 1992, Jurassic and Cretaceous paleomagnetic data from the Southern Alps (Italy): Tectonics, v. 11, p. 811–822.

Clyde, W.C., and Gingerich, P.D., 1998, Mammalian community response to the latest Paleocene thermal maximum: An isotaphonomic study in the northern Bighorn Basin: Geology, v. 27, p. 699–702.

Coccioni, R., Di Leo, R., Galeotti, S., and Monechi, S., 1994, Integrated biostratigraphy and benthic foraminiferal faunal turnover across the Paleocene-Eocene boundary at Trabakua Pass section, northern Spain: Palaeopelagos, v. 4, p. 87–100.

Colosimo, A.B., Bralower, T.J., and Zachos, J.C., 2006, Evidence of lysocline shoaling at the Paleocene/Eocene thermal maximum on Shatsky Rise, northwest Pacific, *in* Bralower, T.J., et al., Proceedings of the Ocean Drilling Program, Scientific Results, Volume 198: College Station, Texas, Ocean Drilling Program, p. 1–36. (Available from World Wide Web: http://www-odp.tamu.edu/publications/198_SR/VOLUME/Chapters/112.PDF.)

Corfield, R.M., 1994, Palaeocene oceans and climate: An isotopic perspective: Earth-Science Reviews, v. 37, p. 225–252, doi: 10.1016/0012-8252(94)90030-2.

Corfield, R.M., and Cartlidge, J.E., 1992, Oceanographic and climatic implications of the Paleocene carbon isotope maximum: Terra Nova, v. 4, p. 443–445.

Corfield, R.M., Cartlidge, J.E., Premoli-Silva, I., and Housley, R.A., 1991, Oxygen and carbon isotope stratigraphy of the Palaeogene and Cretaceous limestones in the Bottaccione Gorge and the Contessa Highway sections, Umbria, Italy: Terra Nova, v. 3, p. 414–422.

Costa, V., Doglioni, C., Grandesso, P., Masetti, D., Pellegrini, G.B., and Tracanella, E., 1996, Carta Geologica d'Italia, Foglio 063, Belluno: Roma, Servizio Geologico d'Italia, scale 1:50,000, 1 sheet + 74 p.

Cramer, B.S., 2001, Latest Paleocene–earliest Eocene cyclostratigraphy using core photographs for reconnaissance geophysical logging: Earth and Planetary Science Letters, v. 186, p. 231–244, doi: 10.1016/S0012-821X(01)00249-7.

Cramer, B.S., and Kent, D.V., 2005, Bolide summer: The Paleocene/Eocene thermal maximum as a response to an extraterrestrial trigger: Palaeogeography, Palaeoclimatology, Palaeoecology, v. 224, p. 144–166, doi: 10.1016/j.palaeo.2005.03.040.

Crouch, E.M., Dickens, G.R., Brinkhuis, H., Aubry, M.-P., Hollis, C.J., Rogers, K.M., and Visscher, H., 2003, The *Apectodinium* acme and terrestrial discharge during the Paleocene-Eocene thermal maximum: New palynological, geochemical and calcareous nannoplankton observations at Tawanui, New Zealand: Palaeogeography, Palaeoclimatology, Palaeoecology, v. 194, p. 387–403, doi: 10.1016/S0031-0182(03)00334-1.

Desio, A., 1974, Geologia d'Italia: Torino, Utet, 1084 p.

D'Hondt, S., Donaghay, P., Zachos, J.C., Luttenberg, D., and Lindinger, M., 1998, Organic carbon fluxes and ecological recovery from the Cretaceous-Tertiary mass extinction: Science, v. 282, p. 276–279, doi: 10.1126/science.282.5387.276.

Dickens, G.R., 1999, The blast in the past: Nature, v. 401, p. 752–755, doi: 10.1038/44486.

Dickens, G.R., 2000, Methane oxidation during the late Paleocene thermal maximum: Bulletin de la Société Géologique de France, v. 171, p. 37–49.

Dickens, G.R., 2001, Carbon addition and removal during the late Palaeocene thermal maximum: Basic theory with a preliminary treatment of the isotope record at ODP Site 1051, Blake Nose, *in* Kroon, D., et al., eds., Western North Atlantic Palaeogene and Cretaceous Palaeoceanography: Geological Society of London Special Publication 183, p. 293–305.

Dickens, G.R., O'Neil, J.R., Rea, D.K., and Owen, R.M., 1995, Dissociation of oceanic methane hydrate as a cause of the carbon isotope excursion at the end of the Paleocene: Paleoceanography, v. 10, p. 965–971, doi: 10.1029/95PA02087.

Dickens, G.R., Castillo, M.M., and Walker, J.C.G., 1997, A blast of gas in the latest Paleocene: Simulating first-order effects of massive dissociation of oceanic methane hydrate: Geology, v. 25, p. 259–262, doi: 10.1130/0091-7613(1997)025<0259:ABOGIT>2.3.CO;2.

Dickens, G.R., Fewless, T., Thomas, E., and Bralower, T.J., 2003, Excess barite accumulation during the Paleocene-Eocene thermal maximum: Massive input of dissolved barium from seafloor gas hydrate reservoirs, *in* Wing, S.L., et al., eds., Causes and Consequences of Globally Warm Climates in the Early Paleogene: Geological Society of America Special Paper 369, p. 11–23.

Di Napoli Alliata, E., Proto Decima, F., and Pellegrini, G.B., 1970, Studio Geologico, Stratigrafico e Micropaleontologico dei Dintorni di Belluno: Memorie della Società Geologica Italiana, v. 9, p. 1–28.

Dinarès-Turell, J., Baceta, J.I., Pujalte, V., Orue-Extebarria, X., and Bernaola, G., 2002, Magnetostratigraphic and cyclostratigraphic calibration of a prospective Paleocene/Eocene stratotype at Zumaia (Basque Basin, northern Spain): Terra Nova, v. 14, p. 371–378, doi: 10.1046/j.1365-3121.2002.00431.x.

Doglioni, C., and Bosellini, A., 1987, Eoalpine and mesoalpine tectonics in the Southern Alps: Geologische Rundschau, v. 77, p. 734–754.

Dolenec, T., Pavšič, J., and Lojen, S., 2000, Ir anomalies and other elemental markers near the Palaeocene-Eocene boundary in a flysch sequence from the western Tethys (Slovenia): Terra Nova, v. 12, p. 199–204, doi: 10.1046/j.1365-3121.2000.00292.x.

Dupuis, C., Aubry, M.-P., Steurbaut, E., Berggren, W., Ouda, K., Magioncalda, R., Cramer, B.S., Kent, D.V., Speijer, R.P., and Heilmann-Clausen, C., 2003, The Dababiya Quarry section: Lithostratigraphy, geochemistry and paleontology, *in* Ouda, K., and Aubry, M.P., eds., The Upper Paleocene–lower Eocene of the Upper Nile Valley: Part 1, Stratigraphy: Micropaleontology, v. 49, supp. 1, p. 41–59.

Dymond, J., Suess, E., and Lyle, M., 1992, Barium in deep-sea sediment: A geochemical proxy for paleoproductivity: Palaeoceanography, v. 7, p. 163–181.

Egger, H., Homayoun, M., Huber, H., Rögl, F., and Schmitz, B., 2005, Early Eocene climatic, volcanic, and biotic events in the northwestern Tethyan Untersberg section, Austria: Palaeogeography, Palaeoclimatology, Palaeoecology, v. 217, p. 243–264, doi: 10.1016/j.palaeo.2004.12.006.

Farley, K.A., and Eltgroth, S.F., 2003, An alternative age model for the Paleocene-Eocene thermal maximum using extraterrestrial $^{3}$He: Earth and Planetary Science Letters, v. 208, p. 135–148, doi: 10.1016/S0012-821X(03)00017-7.

Faul, K.L., and Paytan, A., 2005, Phosphorus and barite concentrations and geochemistry in Site 1221 Paleocene/Eocene boundary sediments, *in* Wilson, P.A., et al., Proceedings of the Ocean Drilling Program, Scientific results, Volume 199: http://www-odp.tamu.edu/publications/199_SR/214/214.htm (accessed February 2006).

Fornaciari, E., Giusberti, L., Luciani, V., Tateo, F., Agnini, C., Backman, J., Oddone, M., and Rio, D., 2007, An expanded Cretaceous-Tertiary transition in a pelagic setting of the Southern Alps (central-western Tethys): Palaeogeography, Palaeoclimatology, Palaeoecology (in press).

Galeotti, S., Angori, E., Coccioni, R., Ferrari, G., Galbrun, B., Monechi, S., Premoli Silva, I., Speijer, R.P., and Turi, B., 2000, Integrated stratigraphy across the Paleocene/Eocene boundary in the Contessa Road section, Gubbio (central Italy): Bulletin de la Société Géologique de France, v. 171, p. 355–365, doi: 10.2113/171.3.355.

Galeotti, S., Kaminski, M.A., Coccioni, R., and Speijer, R.P., 2004, High resolution deep water agglutinated foraminiferal record across the Paleocene/Eocene transition in the Contessa Road section (central Italy), *in* Bubik, M., and Kaminski, M.A., eds., Proceedings of the Sixth International Workshop on Agglutinated Foraminifera: Grzybowski Foundation Special Publication, v. 8, p. 83–103.

Gavrilov, Y.O., Shcherbinina, E.A., and Oberhänsli, H., 2003, Paleocene-Eocene boundary events in the northeastern Peri-Tethys *in* Wing, S.L., et al., eds., Causes and Consequences of Globally Warm Climates in the Early Paleogene: Geological Society of America Special Paper 369, p. 147–168.

Gibson, T.G., Bybell, L.M., and Owens, J.P., 1993, Latest Paleocene lithologic and biotic events in neritic deposits of southwestern New Jersey: Paleoceanography, v. 8, no. 4, p. 495–514.

Gingerich, P.D., 2003, Mammalian response to climate change at the Paleocene-Eocene boundary: Polecat Bench record in the northern Bighorn Basin, Wyoming *in* Wing, S.L., et al., eds., Causes and Consequences of Globally Warm Climates in the Early Paleogene: Geological Society of America Special Paper 369, p. 463–478.

Gingerich, P.D., 2004, Paleogene vertebrates and their response to environmental change, *in* Luterbacher, H.P., ed., Contribution to the Stratigraphy of the Paleogene: Neues Jahrbuch für Geologie und Paläontologie, v. 234, p. 1–23.

Hancock, H.J.L., Dickens, G., Strong, C.P., Hollis, C.J., and Field, B.D., 2003, Foraminiferal and carbon isotope stratigraphy through the Paleocene-Eocene transition at Dee Stream, Marlborough, New Zealand: New Zealand Journal of Geology and Geophysics, v. 46, p. 1–19.

Hollis, C.J., Dickens, G., Field, B.D., Jones, C.M., and Strong, C.P., 2005, The Paleocene–Eocene transition at Mead Stream, New Zealand: A southern Pacific record of early Cenozoic global change: Palaeogeography, Palaeoclimatology, Palaeoecology, v. 215, p. 313–343, doi: 10.1016/j.palaeo.2004.09.011.

Huber, M., and Sloan, L.C., 1999, Warm climate transitions: A general circulation modeling study of the late Paleocene thermal maximum (~56 Ma): Journal of Geophysical Research, v. 104, p. 16,633–16,655, doi: 10.1029/1999JD900272.

Huber, M., and Sloan, L.C., 2000, Climatic responses to tropical sea surface temperature changes on a "greenhouse" Earth: Paleoceanography, v. 15, p. 443–450, doi: 10.1029/1999PA000455.

Jones, B., and Manning, D.A.C., 1994, Comparison of geochemical indices used for the interpretation of palaeoredox conditions in ancient mudstones: Chemical Geology, v. 111, p. 111–194, doi: 10.1016/0009-2541(94)90085-X.

Kaiho, K., Arinobu, T., Ishiwatari, R., Morgans, H.E.G., Okada, H., Takeda, N., Tazaki, K., Zhou, G., Kajiwara, Y., Matsumoto, R., Hirai, A., Niitsuma, N., and Wada, H., 1996, Latest Paleocene benthic foraminiferal extinction and environmental changes at Tawanui, New Zealand: Paleoceanography, v. 11, p. 447–465, doi: 10.1029/96PA01021.

Kaminski, M.A., Gradstein, F.M., Berggren, W.A., Geroch, S., and Beckmann, J.P., 1988, Flysch-type agglutinated foraminiferal assemblages from Trinidad: Taxonomy, stratigraphy and paleobathymetry, *in* Gradstein, M., and Rögl, F., eds., Proceedings of the Second Workshop on Agglutinated Foraminifera, Vienna 1986: Abhandlungen der Geologischen Bundesanstalt, v. 41, p. 155–227.

Katz, M.E., Pak, D.K., Dickens, G.R., and Miller, K.G., 1999, The source and fate of massive carbon input during the latest Paleocene thermal maximum: Science, v. 286, p. 1531–1533, doi: 10.1126/science.286.5444.1531.

Kelly, D.C., 2002, Response of Antarctic (ODP) planktonic foraminifera to the Paleocene-Eocene thermal maximum: Faunal evidence for ocean/climate change: Paleoceanography, v. 17, p. 1071, doi: 10.1029/2002PA000761, doi: 10.1029/2002PA000761.

Kelly, D.C., Bralower, T.J., Zachos, J.C., Premoli Silva, I., and Thomas, E., 1996, Rapid diversification of planktonic foraminifera in the tropical Pacific (ODP Site 865) during the late Paleocene thermal maximum: Geology, v. 24, p. 423–426, doi: 10.1130/0091-7613(1996)024<0423:RDOPFI>2.3.CO;2.

Kelly, D.C., Zachos, J.C., Bralower, T.J., and Schellenberg, S.A., 2005, Enhanced terrestrial weathering/runoff and surface ocean carbonate production during the recovery stages of the Paleocene-Eocene thermal maximum: Paleoceanography, v. 20, p. PA4023, doi: 10.1029/2005PA001163.

Kennett, J.P., and Stott, L.D., 1990, Proteus and proto-Oceanus: Ancestral Paleogene oceans as revealed from Antarctic stable isotopic results: Proceedings of the Ocean Drilling Program, Scientific results, v. 113, p. 865–880.

Kennett, J.P., and Stott, L.D., 1991, Abrupt deep-sea warming, palaeoceanographic changes and benthic

extinctions at the end of the Palaeocene: Nature, v. 353, p. 225–229, doi: 10.1038/353225a0.

Kent, D.V., Cramer, B.S., Lanci, L., Wang, D., Wright, J.D., and Van der Voo, R., 2003, A case for a comet impact trigger for the Paleocene/Eocene thermal maximum and carbon isotope excursion: Earth and Planetary Science Letters, v. 211, p. 13–26, doi: 10.1016/S0012-821X(03)00188-2.

Knox, R.W.O'B., 1998, Kaolinite influx within the Paleocene/Eocene boundary strata of western Europe (extended abstract): Newsletters on Stratigraphy, v. 36, p. 49–53.

Koch, P.L., Zachos, J.C., and Gingerich, P.D., 1992, Correlation between isotope records in marine and continental carbon reservoirs near the Palaeocene/Eocene boundary: Nature, v. 358, p. 319–322, doi: 10.1038/358319a0.

Krumm, S., 1994, WINFIT1.0—A public domain program for interactive profile-analysis under WINDOWS. XIIIth Conference on Clay Mineralogy and Petrology, Praha 1994: Acta Universitatis Carolinae Geologica, v. 38, p. 253–261.

Lourens, L.J., Sluijs, A., Kroon, D., Zachos, J.C., Thomas, E., Röhl, U., Bowles, J., and Raffi, I., 2005, Astronomical pacing of late Palaeocene to early Eocene global warming events: Nature, v. 435, p. 1083–1087, doi: 10.1038/nature03814.

Lu, G., Keller, G., Adatte, T., Ortiz, N., and Molina, E., 1996, Long-term ($10^5$) or short-term ($10^3$) $\delta^{13}C$ excursion near the Palaeocene-Eocene transition: Evidence from the Tethys: Terra Nova, v. 8, p. 347–355.

Lu, G., Adatte, T., Keller, G., and Ortiz, N., 1998, Abrupt climatic, oceanographic and ecologic changes near the Paleocene-Eocene transition in the deep Tethys basin: The Alamedilla section, southern Spain: Eclogae Geologicae Helvetiae, v. 91, p. 293–306.

Luterbacher, H.P., Hardenbol, J., and Schmitz, B., 2000, Decision of the voting members of the International Subcommission on Paleogene Stratigraphy on the criterion of recognition of the Paleocene/Eocene boundary: Newsletter of the International Subcommission on Paleogene Stratigraphy, v. 9, p. 13.

Lyle, M., Wilson, P.A., Janecek, T.R., et al., 2002, Proceedings of the Ocean Drilling Program, Initial reports, Volume 199, http://www-odp.tamu.edu/publications/199_IR/199ir.htm (accessed February 2006).

Martini, E., 1971, Standard Tertiary and Quaternary calcareous nannoplankton zonation, *in* Farinacci, A., ed., Proceedings of the II Plankton Conference, Roma: Roma, Edizioni Tecnoscienza, p. 739–785.

Matsumoto, R., 1995, Cause of the $\delta^{13}C$ anomalies of carbonates and a new paradigm "gas-hydrate hypothesis": Journal of the Geological Society of Japan, v. 101, p. 902–924.

Merriman, R.J., and Peacord, D.R., 1999, Very low-grade metapelites: Mineralogy, microfabrics and measuring reaction progresses, *in* Frey, M., and Robinson, D., eds., Low-Grade Metamorphism: Oxford, UK, Blackwell Scientific, p. 10–60.

Molina, E., Arenillas, I., and Pardo, E., 1999, High resolution planktic foraminiferal biostratigraphy and correlation across the Paleocene/Eocene boundary in the Tethys: Bulletin de la Société Géologique de France, v. 174, p. 521–530.

Monechi, S., and Thierstein, H.R., 1985, Late Cretaceous–Eocene nannofossil and magnetostratigraphic correlations near Gubbio, Italy: Marine Micropaleontology, v. 9, p. 419–440, doi: 10.1016/0377-8398(85)90009-X.

Moore, D.M., and Reynolds, R.C., Jr., 1997, X-ray Diffraction and the Identification and Analysis of Clay Minerals: Oxford, Oxford University Press, 378 p.

Moore, T.C., Jr., Rabinowitz, P.D., et al., 1984, Initial Reports of the Deep Sea Drilling Project, Volume 74: Washington, D.C., U.S. Government Printing Office, xxii + 894 p.

Morford, J.L., and Emerson, S., 1999, The geochemistry of redox sensitive trace metals in sediments: Geochimica et Cosmochimica Acta, v. 63, p. 1735–1750, doi: 10.1016/S0016-7037(99)00126-X.

Norris, R.D., and Röhl, U., 1999, Carbon cycling and chronology of climate warming during the Palaeocene/Eocene transition: Nature, v. 401, p. 775–778, doi: 10.1038/44545.

Norris, R.D., Kroon, D., Klaus, A., et al., 1998, Proceedings of the Ocean Drilling Program, Initial reports, Volume 171B, http://www-odp.tamu.edu/publications/171B_IR/171BTOC.HTM (accessed February 2006).

Oberhänsli, H., 1992, The influence of the Tethys on the bottom waters of the early Tertiary ocean, *in* Kennett, J.P., ed., The Antarctic Paleoenvironment: A Perspective on Global Change: Antarctic Research Series, v. 56, p. 167–184.

Oberhänsli, H., and Hsü, K.J., 1986, Paleocene-Eocene paleoceanography: South Atlantic paleoceanography: Geodynamic Series, v. 15, p. 85–100.

Oddone, M., Genova, N., and Meloni, S., 1986, An accurate procedure for the determination of low levels of iridium in standard reference materials by neutron activation analysis: Journal of Radioanalytical and Nuclear Chemistry, v. 99, p. 325–330, doi: 10.1007/BF02037592.

Ortiz, N., 1995, Differential patterns of benthic foraminiferal extinctions near the Paleocene/Eocene boundary in the North Atlantic and the western Tethys: Marine Micropaleontology, v. 26, p. 341–359, doi: 10.1016/0377-8398(95)00039-9.

Orue-Extebarria, X., Apellaniz, E., Baceta, J.J., Coccioni, R., Di Leo, R., Dinarès-Turell, J., Galeotti, S., Monechi, S., Núñez-Betelu, K., Pares, J.M., Payros, A., Pujalte, V., Samso, J.M., Serra-Kiel, J., Schmitz, B., and Tosquella, J., 1996, Physical and biostratigraphic analysis of two prospective Paleocene-Eocene boundary stratotypes in the intermediate-deep water Basque Basin, western Pyrenees: The Trabakua Pass and Ermua sections: Neues Jahrbuch für Geologie und Palaontologie Abhandlungen, v. 201, p. 179–242.

Pak, D.K., and Miller, K.G., 1992, Paleocene to Eocene benthic foraminiferal isotopes and assemblages: Implications for deepwater circulation: Paleoceanography, v. 7, p. 405–422.

Pälike, H., Laskar, J., and Shackleton, N.J., 2004, Geological constraints on the chaotic diffusion of the Solar System: Geology, v. 32, p. 929–932, doi: 10.1130/G20750.1.

Paytan, A., Kastner, M., Martin, E.E., Macdougall, J.D., and Herbert, T., 1993, Marine barite as a monitor of seawater strontium isotope composition: Nature, v. 366, p. 445–449, doi: 10.1038/366445a0.

Paytan, A., Mearon, S., Cobb, K., and Kastner, M., 2002, Origin of marine barite deposits: Sr and S isotope characterization: Geology, v. 30, p. 747–750, doi: 10.1130/0091-7613(2002)030<0747:OOMBDS>2.0.CO;2.

Perch-Nielsen, K., 1985, Cenozoic calcareous nannoplancton, *in* Bolli, H., Saunders, J.B., and Perch-Nielsen, K., eds., Plankton Stratigraphy: Cambridge, Cambridge University Press, p. 427–554.

Poletti, L., Premoli Silva, I., Masetti, D., Pipan, M., and Claps, M., 2004, Orbitally driven fertility cycles in the Palaeocene pelagic sequences of the Southern Alps (northern Italy): Sedimentary Geology, v. 164, p. 35–54, doi: 10.1016/j.sedgeo.2003.09.001.

Raffi, I., Backman, J., and Pälike, H., 2005, Changes in calcareous nannofossil assemblages across the Paleocene/Eocene transition from the paleo-equatorial Pacific Ocean: Palaeogeography, Palaeoclimatology, Palaeoecology, v. 226, p. 93–126, doi: 10.1016/j.palaeo.2005.05.006.

Ravizza, G., Norris, R.N., Blusztajn, J., and Aubry, M.-P., 2001, An osmium isotope excursion associated with the late Paleocene thermal maximum: Evidence of intensified chemical weathering: Paleoceanography, v. 16, p. 155–163, doi: 10.1029/2000PA000541.

Rio, D., Raffi, I., and Villa, G., 1990, Pliocene-Pleistocene calcareous nannofossil distribution patterns in the western Mediterranean, *in* Kastens, K.A., Mascle, J., et al., Proceedings of the Ocean Drilling Program, Scientific results, Volume 107: College Station, Texas, Ocean Drilling Program, p. 513–533.

Robert, C., and Kennett, J.P., 1994, Antarctic subtropical humid episode at the Paleocene-Eocene boundary: Clay-mineral evidence: Geology, v. 22, p. 211–214, doi: 10.1130/0091-7613(1994)022<0211:ASHEAT>2.3.CO;2.

Röhl, U., Bralower, T.J., Norris, R.D., and Wefer, G., 2000, New chronology for the late Paleocene thermal maximum and its environmental implications: Geology, v. 28, p. 927–930, doi: 10.1130/0091-7613(2000)028<0927:NCFTLP>2.3.CO;2.

Schimper, W.P., 1874, Traité de Paléontologie Végétale, Volume 3: Paris, J.B. Baillière, 896 p.

Schmitz, B., and Pujalte, V., 2003, Sea-level, humidity, and land-erosion records across the initial Eocene thermal maximum from a continental-marine transect in northern Spain: Geology, v. 31, p. 689–692, doi: 10.1130/G19527.1.

Schmitz, B., Charisi, S.D., Thompson, E.I., and Speijer, R.P., 1997a, Barium, $SiO_2$ (excess), and $P_2O_5$ as proxies of biological productivity in the Middle East during the Palaeocene and the latest Palaeocene benthic extinction event: Terra Nova, v. 9, p. 95–99.

Schmitz, B., Asaro, F., Molina, E., Monechi, S., von Salis, K., and Speijer, R.P., 1997b, High-resolution iridium, $\delta^{13}C$, $\delta^{18}O$, foraminifera and nannofossil profiles across the latest Paleocene benthic extinction event at Zumaya, Spain: Palaeogeography, Palaeoclimatology, Palaeoecology, v. 133, p. 49–68, doi: 10.1016/S0031-0182(97)00024-2.

Schmitz, B., Molina, E., and von Salis, K., 1998, The Zumaya section in Spain: A possible global stratotype section for the Selandian and Thanetian Stages: Newsletters on Stratigraphy, v. 36, p. 35–42.

Schmitz, B., Pujalte, V., and Núñez-Betelu, K., 2001, Climate and sea-level perturbations during the initial Eocene thermal maximum: Evidence from siliciclastic units in the Basque Basin (Ermua, Zumaia and Trabakua Pass), northern Spain: Palaeogeography, Palaeoclimatology, Palaeoecology, v. 165, p. 299–320, doi: 10.1016/S0031-0182(00)00167-X.

Schmitz, B., Peucker-Ehrenbrink, B., Heilmann-Clausen, C., Aberg, G., Asaro, F., and Lee, C.-T.A., 2004, Basaltic explosive volcanism, but no comet impact, at the Paleocene-Eocene boundary: High-resolution chemical and isotopic records from Egypt, Spain and Denmark: Earth and Planetary Science Letters, v. 225, p. 1–17, doi: 10.1016/j.epsl.2004.06.017.

Shackleton, N.J., 1986, Paleogene stable isotope events: Palaeogeography, Palaeoclimatology, Palaeoecology, v. 57, p. 91–102, doi: 10.1016/0031-0182(86)90008-8.

Shackleton, N.J., 1987, The carbon isotope record of the Cenozoic: History of organic carbon burial and of oxygen in the ocean and atmosphere, *in* Brooks, J., and Fleet, A.J., eds., Marine Petroleum Source Rocks: Geological Society of London Special Publication 26, p. 423–434.

Shackleton, N.J., and Hall, M.A., 1984, Carbon isotope data from Leg 74 sediments, *in* Moore, T.C., Jr., Rabinowitz, P.D., et al., Initial Reports of the Deep Sea Drilling Project, Volume 74: Washington, D.C., U.S. Government Printing Office, p. 613–619.

Shackleton, N.J., Hall, M.A., and Bleil, U., 1985, Carbon-isotope stratigraphy, Site 577, *in* Heat, G.R., Burkle, L.H., et al., Initial Reports Deep Sea Drilling Project, Volume 86: Washington, D.C., U.S. Government Printing Office, p. 503–511.

Speijer, R.P., and Wagner, T., 2002, Sea-level changes and black shales associated with the late Paleocene thermal maximum: Organic-geochemical and micropaleontological evidence from the southern Tethyan margin (Egypt-Israel), *in* Koeberl, C., and MacLeod, K.G., eds., Catastrophic Events and Mass Extinctions: Impacts and Beyond: Geological Society of America Special Paper 356, p. 533–549.

Speijer, R.P., Schmitz, B., and van der Zwaan, G.J., 1997, Benthic foraminiferal extinction and repopulation in response to latest Paleocene Tethyan anoxia: Geology, v. 25, p. 683–686, doi: 10.1130/0091-7613(1997)025<0683:BFEARI>2.3.CO;2.

Stefani, C., and Grandesso, P., 1991, Studio preliminare di due sezioni del Flysch bellunese: Rendiconti della Società Geologica Italiana, v. 14, p. 157–162.

Stoll, H.M., 2004, Reply to comment by Timothy J. Bralower, D. Clay Kelly, and Deborah J. Thomas on "Coccolith Sr/Ca records of productivity during the Paleocene-Eocene thermal maximum from the Weddell Sea": Paleoceanography, v. 19, p. PA1015, doi: 10.1029/2003PA000971.

Stoll, H.M., 2005, Limited range of interspecific vital effects in coccolith stable isotopic records during the Paleocene-Eocene thermal maximum: Paleoceanography, v. 20, p. PA1007, doi: 10.1029/2004PA001046.

Stott, L.D., Sinha, A., Thiry, M., Aubry, M.-P., and Berggren, W.A., 1996, Global $\delta^{13}C$ changes across the Paleocene/Eocene boundary: Criteria for terrestrial-marine correlations, *in* Knox, R.W.O'B., et al., eds., Correlation of the Late Paleocene–Early Eocene in Northwest

Europe: Geological Society of London Special Publication 101, p. 381–399.
Taylor, S.R., and McLennan, S.M., 1985, The Continental Crust: Its Composition and Evolution: Oxford, UK, Blackwell Scientific Publications, 312 p.
Thiry, M., 2000, Palaeoclimatic interpretation of clay minerals in marine deposits: An outlook from the continental origin: Earth-Science Reviews, v. 49, p. 201–221, doi: 10.1016/S0012-8252(99)00054-9.
Thomas, D.J., Bralower, T.J., and Zachos, J.C., 1999, New evidence for subtropical warming during the late Paleocene thermal maximum: Stable isotopes from Deep Sea Drilling Project Site 527: Walvis Ridge: Paleoceanography, v. 14, p. 561–570, doi: 10.1029/1999PA900031.
Thomas, D.J., Zachos, J.C., Bralower, T.J., Thomas, E., and Bohaty, S., 2002, Warming the fuel for the fire: Evidence for the thermal dissociation of methane hydrate during the Paleocene-Eocene thermal maximum: Geology, v. 30, p. 1067–1070, doi: 10.1130/0091-7613(2002)030<1067:WTFFTF>2.0.CO;2.
Thomas, E., 1998, Biogeography of the late Paleocene benthic foraminiferal extinction, *in* Aubry, M.-P., et al., eds., Late Paleocene–Early Eocene Climatic and Biotic Events in the Marine and Terrestrial Records: New York, Columbia University Press, p. 214–243.
Thomas, E., 2003, Extinction and food at the seafloor: A high-resolution benthic foraminiferal record across the initial Eocene thermal maximum, Southern Ocean Site 690, *in* Wing, S.L., et al., eds., Causes and Consequences of Globally Warm Climates in the Early Paleogene: Geological Society of America Special Paper 369, p. 319–332.
Thomas, E., and Shackleton, N.J., 1996, The Paleocene-Eocene benthic foraminiferal extinction and stable isotope anomalies, *in* Knox, R.W.O'B., et al., eds., Correlation in the Early Paleogene in Northwest Europe: Geological Society of London Special Publication 101, p. 401–441.
Thompson, E.I., and Schmitz, B., 1997, Barium and the late Paleocene $\delta^{13}C$ maximum: Evidence of increased marine surface productivity: Paleoceanography, v. 12, p. 239–254, doi: 10.1029/96PA03331.
Tjalsma, R.C., and Lohmann, G.P., 1983, Paleocene-Eocene bathyal and abyssal benthic foraminifera from the Atlantic Ocean: Micropaleontology Special Publication, v. 4, p. 1–90.
Tripati, A., and Elderfield, H., 2004, Abrupt hydrographic changes in the equatorial Pacific and subtropical Atlantic from foraminiferal Mg/Ca indicate greenhouse origins for the thermal maximum at the Paleocene-Eocene boundary: Geochemistry, Geophysics, Geosystems, v. 5, p. Q02006, doi: 10.1029/2003GC000631.
Turekian, K.K., and Wedepohl, K.H., 1961, Distribution of the elements in some major units of the Earth's crust: Geological Society of America Bulletin, v. 12, p. 175–192.
Van Morkhoven, F.P.C.M., Berggren, W.A., and Edwards, A.S., 1986, Cenozoic cosmopolitan deep-water benthic foraminifera: Bulletin des Centres de Recherches Exploration–Production Elf-Aquitanie, Mémoire, v. 11, 421 p.
Walker, J.C.G., Hays, P.B., and Kasting, J.F., 1981, A negative feedback mechanism for the long-term stabilization of Earth's surface temperature: Journal of Geophysical Research, v. 86, p. 9776–9782.
Weedon, G.P., Shackleton, N.J., and Pearson, P.N., 1997, The Oligocene time scale and cyclostratigraphy on the Ceara Rise, western equatorial Atlantic, *in* Shackleton, N.J., Curry, W.B., Richter, C., and Bralower, T.J., et al., Proceedings of the Ocean Drilling Program, Scientific results, Volume 154: College Station, Texas, Ocean Drilling Program, p. 101–114.
Winterer, E.L., and Bosellini, A., 1981, Subsidence and sedimentation on Jurassic passive continental margin, Southern Alps, Italy: American Association of Petroleum Geologists Bulletin, v. 65, p. 394–421.
Zachos, J.C., and Dickens, G.R., 2000, An assessment of the biogeochemical feedback response to the climatic and chemical perturbations of the LPTM: Geologiska Föreningens i Stockholm Förhandlingar (GFF), v. 122, p. 188–189.
Zachos, J.C., Lohmann, K.C., Walker, J.C.G., and Wise, S.W., 1993, Abrupt climate change and transient climates during the Paleogene: A marine perspective: The Journal of Geology, v. 101, p. 191–213.
Zachos, J.C., Pagani, M., Sloan, L.C., Thomas, E., and Billups, K., 2001, Trends, rhythms, and aberrations in global climate 65 Ma to present: Science, v. 292, p. 686–693, doi: 10.1126/science.1059412.
Zachos, J.C., Wara, M.W., Bohaty, S., Delaney, M.L., Petrizzo, M.R., Brill, A., Bralower, T.J., and Premoli Silva, I., 2003, A transient rise in tropical sea surface temperature during the Paleocene-Eocene thermal maximum: Science, v. 302, p. 1551–1554, doi: 10.1126/science.1090110.
Zachos, J.C., Kroon, D., Blum, P., et al., 2004, Proceedings of the Ocean Drilling Program, Initial reports, Volume 208, http://www-odp.tamu.edu/publications/208_IR/208ir.htm (accessed February 2006).
Zachos, J.C., Röhl, U., Schellenberg, S.A., Sluijs, A., Hodell, D.A., Kelly, D.C., Thomas, E., Nicolo, M., Raffi, I., Lourens, L.J., McCarren, H., and Kroon, D., 2005, Rapid acidification of the ocean during the Paleocene-Eocene thermal maximum: Science, v. 308, p. 1611–1615, doi: 10.1126/science.1109004.

Manuscript Received 1 March 2006
Revised Manuscript Received 1 September 2006
Manuscript Accepted 14 September 2006

Printed in the USA